Earth-Science Reviews 129 (2014) 59–84

Contents lists available at ScienceDirect

Earth-Science Reviews

journal homepage: www.elsevier.com/locate/earscirev

Review

Continental orogenesis from ocean subduction, continent collision/subduction, to orogen collapse, and orogen recycling: The example of the North Qaidam UHPM belt, NW China

Shuguang Song [a,*], Yaoling Niu [b,c], Li Su [d], Cong Zhang [a], Lifei Zhang [a]

[a] MOE Key Laboratory of Orogenic Belts and Crustal Evolution, School of Earth and Space Sciences, Peking University, Beijing 100871, China
[b] Department of Earth Sciences, Durham University, Durham DH1 3LE, UK
[c] Institute of Oceanology, Chinese Academy of Sciences, Qingdao 266071, China
[d] Institute of Earth Science, Chinese University of Geosciences, Beijing 100083, China

ARTICLE INFO

Article history:
Received 12 May 2013
Accepted 21 November 2013
Available online 4 December 2013

Keywords:
Continental-type UHPM belt
Post-collisional magmatism
Orogenesis and mountain collapse
Decoupling of oceanic and continental subduction belts
Orogen recycling
Northern Tibetan Plateau

ABSTRACT

The North Qaidam ultra-high pressure metamorphic (UHPM) belt in the northern Tibetan Plateau records a complete history of the evolution of a continental orogen from prior seafloor subduction, to continental collision and subduction, and to the ultimate orogen collapse in the time period from the Neoproterozoic to the Paleozoic. Lithologies in this UHPM belt consist predominantly of felsic gneisses containing blocks of eclogite and peridotite. The 1120–900 Ma granitic and psammitic/pelitic gneisses compose the majority of the UHPM belt and is genetically associated with the previous orogenic cycle of Grenville-age, whereas protoliths of the HUPM eclogites are of both the 850–820 Ma continental flood basalts (CFBs) and the 540–500 Ma oceanic crust (ophiolite). The early stage of quartz-stable eclogite-facies metamorphism took place at ~445–473 Ma, the same age as that of the HP rocks in the North Qilian oceanic suture zone, representing the earliest subducting seafloor rocks exhumed and preserved. Coesite-bearing zircons from the metapelite and eclogite, diamond-bearing zircons from garnet peridotites constrain the UHP metamorphic age of ~438–420 Ma, which represents the timing of continental subduction at depths of 100–200 km, ~10–20 m.y. younger than the early stage of the Qilian seafloor subduction. Therefore, deep subduction of continental crust should be the continuation of oceanic subduction that is pulled down by the sinking oceanic lithosphere or pushed down by the overriding upper plate, which is an expected and inevitable consequence for the scenario of passive continental margins. Partial melting of subducted ocean crust might occur in response to continental subduction at ~435 Ma.

The UHPM rocks started to exhume accompanied by mountain building and deposition of Early Devonian molasses in the North Qilian region at ~420 Ma. Decoupling of oceanic subduction zone and continent UHPM terranes may be attributed to the different exhumation path and mechanism between the subducted oceanic and continent crusts, or rollback of subduction zone. Decompression melting of UHP metamorphosed slab and continental crust during exhumation is responsible for the generation of adakitic melts and S-type granite. Mountain collapse and lithosphere extension happened in the period of ~400–360 Ma and formed diorite–granite intrusions in the UHPM belt, which marked the end of a complete orogenic cycle.

This UHP metamorphic belt presents an example of multi-epoch tectonic recycles, represented by recombination of the Neoproterozoic Grenvillian orogenesis and the Early Paleozoic Caledonian orogenesis.

Contents

1. Introduction . . . 60
2. Regional geologic setting . . . 61
   2.1. Alashan Block . . . 61
   2.2. Qilian Block . . . 61
   2.3. Qaidam Block . . . 61
   2.4. North Qilian oceanic-type subduction zone . . . 63
   2.5. North Qaidam UHP belt . . . 63
3. Dulan UHPM terrane . . . 63

* Corresponding author. Tel.: +86 106 276 7729.
E-mail address: sgsong@pku.edu.cn (S.G. Song).

0012-8252/$ – see front matter
http://dx.doi.org/10.1016/j.earscirev.2013.11.010

3.1. Rock assemblage and petrography . . . 63
3.1.1. Eclogite . . . 63
3.1.2. Pelitic and granitic gneisses . . . 65
3.1.3. High-pressure granulite and adakitic melts in the SDB . . . 65
3.2. UHP metamorphosed ophiolitic sequence in the NBD . . . 65
3.2.1. Ophiolite-like sequence in Yematan section . . . 65
3.2.2. Ophiolite sequence in Shaliuhe Section . . . 65
3.3. Protoliths and metamorphic ages for the Dulan UHP rocks . . . 67
3.3.1. Protolith and metamorphic ages of the Shaliuhe ophiolite . . . 67
3.3.2. Metamorphic ages of the NDB pelitic gneisses and eclogite in Yematan . . . 67
3.3.3. Protolith and metamorphic ages of Aerchituoshan coesite-bearing eclogite . . . 67
3.3.4. Protolith and metamorphic ages of the granitic gneisses . . . 67
3.4. Metamorphic evolution and P–T estimations . . . 67
3.4.1. P–T conditions of the NDB . . . 68
3.4.2. P–T conditions of the SDB . . . 68
3.4.3. P–T–t paths of the Dulan UHP terrane . . . 69
4. Xietieshan terrane . . . 69
4.1. Eclogite . . . 69
4.2. Gneisses . . . 69
4.3. Geochronology of the Xitieshan HP-UHP rocks . . . 69
4.3.1. HP-UHP metamorphic ages from eclogite and paragneiss . . . 69
4.3.2. Protolith ages of eclogite and gneisses . . . 70
5. Yuka eclogite terrane . . . 71
5.1. Eclogite . . . 71
5.2. Granitic and psammitic/pelitic gneisses . . . 71
5.3. Ages and geochemistry of the Yuka eclogite . . . 71
5.3.1. UHP metamorphic ages . . . 71
5.3.2. Protolith ages . . . 73
5.3.3. Whole-rock chemistry . . . 73
5.4. Protolith of the Yuka eclogite: implications for onset rifting of the Rodinia supercontinent . . . 73
5.5. Protolith and metamorphic ages of felsic gneisses . . . 74
5.5.1. Protolith ages of granitic gneiss . . . 74
5.5.2. Protolith and metamorphic ages of paragneisses . . . 74
6. Lüliangshan garnet peridotite massif . . . 74
6.1. Occurrence and petrography . . . 75
6.2. Exsolution lamellae in rock-forming minerals . . . 75
6.3. UHP metamorphic ages of the garnet peridotite . . . 76
6.4. Protolith of the Lüliangshan peridotite: material from Grenville-age juvenile mantle? . . . 76
7. Post-collisional magmatic sequences . . . 77
8. Discussion . . . 77
8.1. UHPM protoliths of the subducted complex: records of Grenville orogenesis, Neoproterozoic CFBs and Early Paleozoic ocean crust . . . 77
8.1.1. Granitic gneiss—products of the Grenville-age orogeny . . . 77
8.1.2. Eclogite protoliths—Neoproterozoic CFBs vs. fragments of Early Paleozoic ocean crust . . . 78
8.1.3. UHP pelitic/psammitic gneiss—sediments at a foredeep vs. old paragneisses from the Grenville-age continental crust . . . 78
8.1.4. Two kinds of peridotite blocks—oceanic vs. continental lithospheric mantle . . . 78
8.2. Time constraint for oceanic subduction, continental subduction and exhumation . . . 78
8.2.1. Determination of UHP metamorphic time for continental subduction . . . 78
8.2.2. Oceanic subduction prior to continental collision—two stages of eclogite metamorphism . . . 79
8.2.3. Granulite overprinting and decompression partial melting during exhumation . . . 80
8.2.4. Mountain building, UHP exhumation and decoupling of oceanic subduction zone and continent UHPM terranes . . . 80
8.2.5. Mountain collapse and extensional magmatism . . . 80
8.3. Tectonic evolution from oceanic subduction, to continental collision and to final mountain collapse . . . 81
Acknowledgments . . . 82
References . . . 82

1. Introduction

Orogenic belts preserved in continents have undergone long and complex histories involving continental rifting, ocean floor spreading, seafloor subduction, continental collision/subduction, mountain building and collapse (e.g., Thomas, 1983; Torsvik et al., 1996; Handy et al., 2010). High and ultrahigh-pressure metamorphic rocks within orogenic belts are key recorders of many of these processes (e.g. Ernst, 2001; Chopin, 2003; Liou et al., 2004; Guillot et al., 2009; Brueckner, 2011; Herwartz et al., 2011; Rubatto et al., 2011). On the basis of lithological assemblage of HP-UHP metamorphic rocks, paleo-subduction zones identified within continents can be conveniently divided into oceanic-type and continental-type (Song et al., 2006) although the latter is the continuation of the former following the closure of an ocean basin and continental collision. These divisions are equivalent to the Pacific-type and Alpine-type (Ernst and Liou, 1995; Ernst, 2001) or B-type and A-type (Maruyama et al., 1996) subduction zones in the literature. Table 1 lists the major lithologies in the two end-member types of subduction zones.

Subduction zones in a variety of settings can provide clues for dynamic understandings (e.g., Doglioni et al., 1999; Wortel and Spakman, 2000; Doglioni et al., 2006, 2007; Lucente and Margheriti, 2008). The general notion is that, after seafloor consumption upon continental collision, the continental portion of the same lithosphere (i.e., in the case of passive continental margins) continues to subduct to depths greater than 80 km before exhumation as a result of oceanic lithosphere

Table 1
Comparison of major components of the oceanic-type and continental-type subduction zones.

Oceanic-type	Continental-type
Accretionary complex • Ophiolite suite • Island-arc igneous sequence • Low-T (lawsonite-bearing) blueschist and eclogite (T < 550 °C, P mostly < 2.5 GPa) • Mélange with blocks of pelagic chert, oceanic lithosphere fragments and limestone	Continent crust • Granitic gneiss (~80 vol.%) • Paragneiss and marble (inland and continental margin) • Mediate to high T eclogite (T > 600 °C, P mostly > 2.5 GPa) • Garnet peridotite • Jadeite quartzite

breakoff. This view, if correct, has two prerequisites for the continental deep subduction: (1) prior oceanic lithosphere subduction and (2) this oceanic lithosphere shared by its continental counterpart through the passive margin. The Early Paleozoic Qilian–Qaidam orogeny is interpreted as examples of such processes (e.g. Song et al., 2006). Important new occurrences include the Qilian lawsonite-bearing blueschist and eclogite which required a very cold subduction of the Early Paleozoic oceanic lithosphere, and the mixing of oceanic and supracrustal protoliths in the Qaidam continental subduction channel. These two Early Paleozoic sutures on the northern Tibetan Plateau provide a type example of a complete cycle of continental orogenesis in the context of the regional tectonic evolution of Qilian Ocean (Proto-Tethys vs. branch of Iapetus Ocean) in south-central Asia.

As eclogite and garnet peridotite were reported in 1990's (Yang et al., 1994, 1998), the North Qaidam became one of the newly-recognized ultrahigh-pressure metamorphic (UHPM) belts (e.g., Yang et al., 2001, 2002a,b, 2006; Song et al., 2003a,b, 2004, 2005a,b, 2006; J.X. Zhang et al., 2005; Mattinson et al., 2006a,b, 2007; Xu et al., 2006; Zhang et al., 2006; Yin et al., 2007; J.X. Zhang et al., 2010) and has been listed as the 22nd UHPM belt in the world (Carswell and Compagnoni, 2003). This UHPM belt is temporally similar to the Western Gneiss Region of the Caledonian orogenic belt in Norway and has received much attention over the past decade. A significantly improved understanding of the tectonic evolution of the orogenic belt is now emerging thanks to detailed mineralogical, petrologic, geochemical and geochronological studies as well as field observations carried out over the past ten years. This, together with some new age data of both eclogite and felsic gneisses, allows us to complete the model of continental orogenesis that enriches the Wilson Cycle with added data, new observations and new insights in the Early Paleozoic.

Mineral abbreviations are after Whitney and Evans (2010).

2. Regional geologic setting

The Tibetan Plateau, the "Roof of the World", has long been thought to have formed as a result of the subduction, collision and postcollisional convergence of Paleo- and Neo-Tethys oceans between Gondwana and Laurasia continents (e.g., Tapponnier et al., 2001; Li et al., 2006; Guillot et al., 2008; Royden et al., 2008; Liou et al., 2009; Zhai et al., 2011). The collision and continued northward convergence of the Indian Plate in the early Cenozoic have complicated the tectonic framework of the continental China (e.g. Yin et al., 2008a,b) (Fig. 1).

The Qilian–Qaidam orogenic system at the northern edge of the Tibet Plateau is bounded by the Qaidam Basin to the south, the Tarim Basin to the west, and the Sino-Korean craton to the east (Fig. 1). This region includes various continental blocks, HP and UHP suture zones and metamorphic belts and is offset by the Altyn Tagh fault, one of the largest strike-slip fault systems in the world. The tectono-lithological correlations on both sites of the Altyn Tagh fault have displaced left-laterally the HP and UHP belts by ~400 km of displacement occurred along this profound break (e.g., Zhang et al., 2001). To the east, the Qilian oceanic-type orogen, extends from the Altyn Tagh fault southeastward for ~1000 km to the Qinling–Dabie orogen, and forms a major geographic-tectonic boundary between North and South China (not shown).

The Qilian–Qaidam orogenic system consists of the earliest subduction zones of Caledonian ages in the northern Tibet Plateau. However, this orogenic system is beyond the Tethys tectonic domain, and may represent tectonic evolution of the eastern branch of the worldwide "Iapetus Ocean" between the two continents of Baltica and Laurentia (Song et al., 2013, in revision). Two apparently distinct, sub-parallel subduction zones, i.e., the North Qilian oceanic-type suture zone and the North Qaidam continental-type subduction zone, occur in between three blocks, from north to south, the Alashan Block, the Qilian Block, and the Qaidam Block (Fig. 2).

2.1. Alashan Block

The Alashan Block in the north is generally thought as the western part of the North China Craton (e.g., Zhao et al., 2005). Recent study by Dan et al. (2012) revealed that the primary magmatic ages of the mafic and felsic igneous rocks are at ca. 2.34–2.30 Ga with zircon Hf model ages of 2.92–2.81 Ga, similar to the Qilian block. The ambiguous Archaean nucleus is signified by the ~2.7 Ga amphibolite in the northeast part of the block (Geng et al., 2006), as well as by some 2.5–3.5 Ga detrital zircons from meta-sedimentary sequences (e.g. Tung et al., 2007a). It was intruded by a ~830 Ma Cu–Ni-bearing ultramafic body (Li et al., 2005) and by 845–971 Ma foliated granites (Wan et al., 2001; Geng et al., 2002). These Neoproterozoic intrusions suggested that the Alashan block is unlikely to be the west part of the North China Craton (Dan et al., 2012; Song et al., 2013, in revision).

2.2. Qilian Block

The Qilian Block, located between the North Qilian Suture Zone and the North Qaidam UHP Belt, is an imbricate thrust belt of Precambrian basement overlain by thick and large-area Paleozoic sedimentary sequences. In fact, it is not an integrate block as an ophiolitic and intra-oceanic arc complex belt (namely the Lajishan OIOAB) discontinuously extends along the NW direction (Fig. 2). The Precambrian complexes outcrop in Da Qaidam region in the southwest compose of Paleoproterozoic granitic gneiss (~2.2–2.47 Ma), leucogranite (1.91–1.96 Ga) and rapakivi granites (1.76–1.77 Ga) (Lu, 2002; N.S. Chen et al., 2009; Wang et al., 2009). Granitic intrusions of 880–940 Ma have been identified in gneisses in the north part of the Xining region (Guo et al., 1999; Wan et al., 2001; Tung et al., 2007b), similar to granitic gneisses from the North Qaidam UHP Belt. These data led to the consensus that the Qilian block has close affinities with the Yangtze Craton (e.g., Wan et al., 2001; Gehrels et al., 2003; Darby and Gehrels, 2006; N.S. Chen et al., 2009).

The Lajishan OIOAB composes 525 Ma ophiolite and 460–442 Ma intra-oceanic volcanic rocks (Song et al., unpublished data), which may suggests the final suture zone of the Qilian–Qaidam subduction system. It is remarkable that thick Ordovician–Silurian sedimentary rocks plus minor volcanic rocks deposited in the south part of the Qilian block (Fig. 2), which have been suggested to be formations of miogeosyncline (Ren et al., 1980). It is most likely deposited in a foreland basin system combining sediments from passive margin and the foredeep (e.g., Doglioni, 1994; DeCelles and Giles, 1996).

2.3. Qaidam Block

The Qaidam Block to the south is a Mesozoic to Cenozoic intracontinental basin and deposits thick sedimentary strata that cover most of the block. The Precambrian crystalline basement mainly exposes in the south margin of the Qaidam block (Eastern Kunlun). Wang et al. (2004) confirmed the Grenville-aged (988–1074 Ma)

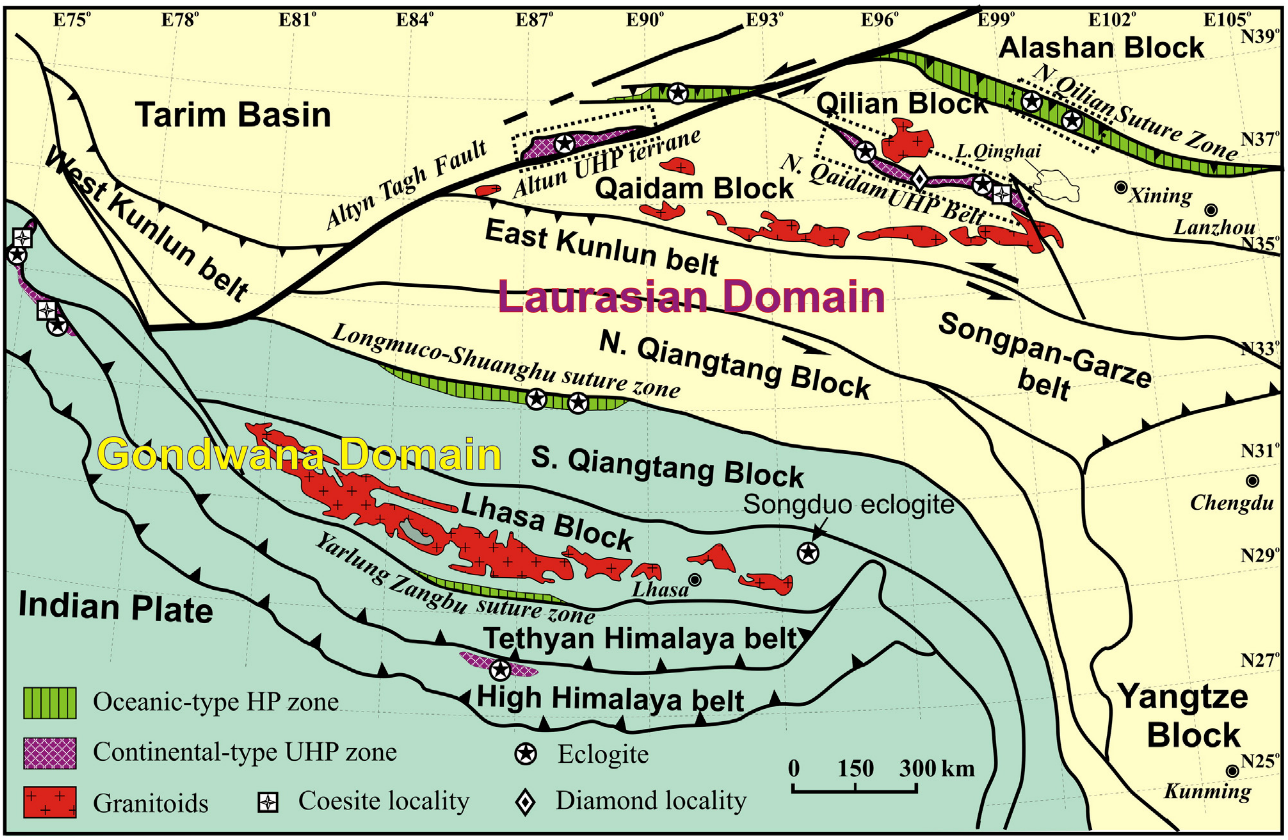

Fig. 1. Distribution of major tectonic units in the Tibetan Plateau; these include various continental blocks, HP and UHP suture zones and metamorphic belts (Modified after Liou et al., 2009).

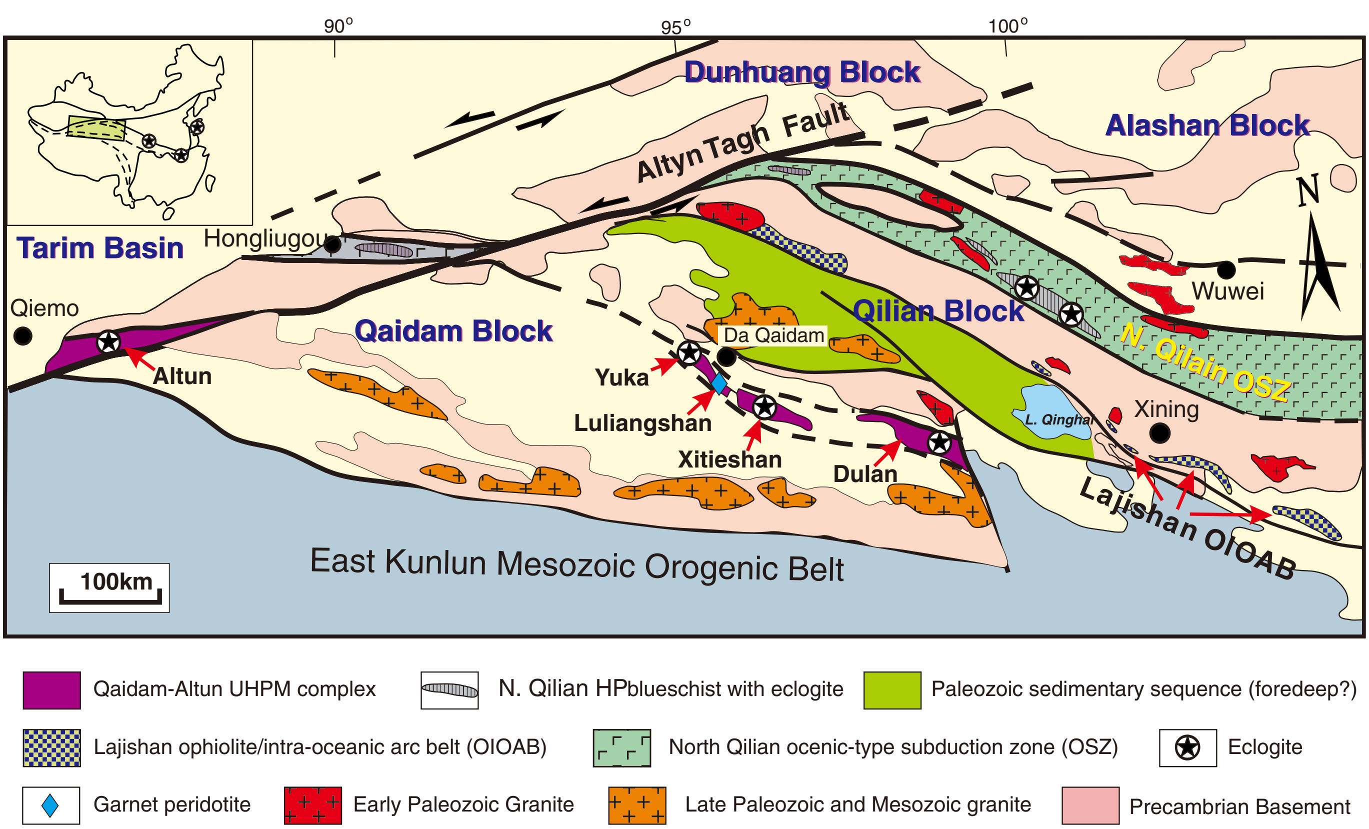

Fig. 2. Schematic maps showing major tectonic subunits of the Qilian–Qaidam orogenic belts in the northern Tibetan Plateau (After Song et al., 2006).

metamorphism and anatexis in pelitic and granitic gneisses and detrital zircons of 2.4–2.6 Ga with rare 3.2 Ga from the southern part of the Qaidam block, and thus concluded that the Qaidam–Qilian Craton has an affinity with the Yangtze Craton.

2.4. North Qilian oceanic-type subduction zone

The North Qilian Suture Zone is an elongate, NW-trending orogenic belt that lies between the Alashan Block (north) and the Qilian Block (south) (Fig. 2). This belt has been considered as a material record of a typical oceanic-type subduction-zone in the early Paleozoic as it comprises mid-ocean-ridge and back-arc-basin ophiolite suites with zircon SHIRMP U–Pb ages of 560–450 Ma, calc-alkaline volcanic (510–450 Ma) and granitic rocks (510–420 Ma), and subduction-zone complexes including HP metamorphic rocks and mélange (for details, see Song et al., 2013, in revision and references therein). Boninitic sequence (517–490 Ma) in the back-arc setting was also determined (Xia et al., 2012).

Recent studies concur with the earlier notion, but emphasize that this belt is an early Paleozoic oceanic suture zone (~440–710 Ma) between the Alashan and the Qilian–Qaidam micro-continents, fragments of the Rodinia supercontinent (Wan et al., 2001; Lu, 2002; Tung et al., 2007b; Song et al., 2012). Wu et al. (1993) reported occurrences of high-grade blueschist with an assemblage of Grt + Gln + Ep + Phn + Ab + Qtz and low-grade blueschist characterized by an assemblage of Gln + Lws + Pmp + Ab + Chl + Arg + Qtz in two distinct areas, and P–T estimates of ~340 °C and 0.8 ± 0.1 GPa for eclogite lenses within high-grade blueschists. Recent findings of lawsonite-bearing eclogite and carpholite-bearing meta-pelite (Song et al., 2007b; Zhang et al., 2007a) afford convincing evidence that the North Qilian HP metamorphic belt records cold oceanic lithosphere subduction with a low geothermal gradient (6–7 °C/km) in the early Paleozoic.

Petrological and geochemical data, together with age dates, reveal that the suture zone rocks record a long tectonic history from ocean floor spreading, to oceanic lithosphere subduction, and to ultimate continental collision and mountain-building in four stages (Song et al., 2009a, 2013, in revision). Stage I (Late Proterozoic to Cambrian): the Rodinia supercontinent broke up and formed the Qilian Ocean in the Late Proterozoic to Cambrian (from 710 Ma (?) to ~520 Ma), separating the Alashan block to the north and the Qilian–Qaidam block to the south. The Qilian–Qaidam block may be a fragment of the disintegrated Rodinia supercontinent with passive margins extending into oceanic lithosphere that floored the Qilian Ocean (Song et al., 2006). Stage II (Late Cambrian to Middle Ordovician): oceanic lithosphere started to subduct northwards beneath western margin of the Alashan block along a cold geotherm of ~6–7 °C/km, and to undergo blueschist- and eclogite-facies metamorphism at the late Cambrian (ca. 520 Ma), accompanied by subduction-zone related mafic to felsic volcanism (e.g., island-arc) and ophiolite in the back-arc basin. Stage III (Late Ordovician to Silurian): the Qilian Ocean closed at the Late Ordovician and the back-arc basin seafloor started to subduct southwards and forms the low-grade blueschist belt. In the Silurian (~440–420 Ma), thick flysch sequence had deposited in a remnant sea. Stage IV (Late Silurian to Early Devonian): continental collision and orogenesis occurred at the Late Silurian and Devonian, which led to the mountain-building and uplifting, and as a result, the lower Devonian molasse deposited.

2.5. North Qaidam UHP belt

The North Qaidam UHPM belt is located between the Qilian Block in the north and the Qaidam Block in the south. It trends WNW and extends from Dulan northwestward, through Xitieshan, Lüliangshan, to Yuka for about 400 km (see Fig. 2) where it is offset from the equivalent Altun UHPM belt by the Altyn Tagh Fault. The North Qaidam/Altun UHPM belt mainly consists of granitic and pelitic gneisses intercalated with blocks of eclogite and varying amounts of ultramafic rocks, especially garnet peridotite. The rock assemblages suggest that this belt is typical of a continental-type subduction zone (Yang et al., 1998, 2001, 2002a,b; Song et al., 2003a,b, 2005a,b, 2006, 2009b,c; G.B. Zhang et al., 2005; J.X. Zhang et al., 2005; Mattinson et al., 2006a,b, 2007, 2009; Zhang et al., 2006; J.X. Zhang et al., 2008; J.X. Zhang et al., 2010; Liu et al., 2012a,b), which differs from the "cold", oceanic-type subduction of the North Qilian suture zone (Wu et al., 1993; J.X. Zhang et al., 2007a; Song et al., 2007a,b, 2009a,b,c,d,e, 2013, in revision).

Coesite inclusions have been identified in zircon and garnet from metapelite and eclogite at Dulan, Xitieshan and Yuka (Yang et al., 2001, 2002a,b; Song et al., 2003a,b, 2006; G.B. Zhang et al., 2009a,b; J.X. Zhang et al., 2009a; J.X. Zhang et al., 2010; Liu et al., 2012a,b) and diamond in zircon from the garnet peridotite at Lüliangshan (Song et al., 2005a), respectively. P–T estimates of the enclosing eclogite and garnet peridotite establish the North Qaidam eclogite belt as an Early Paleozoic UHPM terrane exhumed from depths of 100–200 km (Song et al., 2004, 2005a,b).

3. Dulan UHPM terrane

The Dulan UHPM terrene is located at the southeast end of the North Qaidam UHPM belt. It has been extensively studied in terms of petrology, geochemistry, and zircon geochronology by different groups of authors in the last decade (Song and Yang, 2001; Yang et al., 2001, 2002a,b, 2006; Song et al., 2003a,b, 2006, 2009a,b,c,d,e; G.B. Zhang et al., 2005; Mattinson et al., 2006a,b, 2007, 2009; G.B. Zhang et al., 2008; G.B. Zhang et al., 2009a,b; J.X. Zhang et al., 2009a; Yu et al., 2009, 2010, 2012; J.X. Zhang et al., 2010; C. Zhang et al., 2012). This terrane is the first place where coesite inclusions in zircon grains from metapelite, coesite and coesite-pseudomorphs in eclogite were identified (Song and Yang, 2001; Yang et al., 2001, 2002a,b; Song et al., 2003a,b; G.B. Zhang et al., 2009a,b; J. Zhang et al., 2009a; J.X. Zhang et al., 2010), which corroborated that the North Qaidam is a typical continental subduction complex exhumed from depths >80 to 100 km.

On the basis of spatial relations, and the parageneses and compositions of eclogitic minerals, two distinct sub-belts, namely the South Dulan Belt (SDB) and the North Dulan Belt (NDB), are recognized (Song et al., 2003a; Fig. 3). The northern belt crops out in an area of about 100 km^2; and is partly covered by Quaternary sediments in the east and intruded by a large diorite–granite pluton in the west. The south belt, extending for more than 30 km, is restricted to a belt of 2–5 km wide and bounded by two thrust faults. The Dulan eclogite-bearing terrane consists of eclogite, garnet amphibolite (retrograde eclogite), mafic granulite (granulitized eclogite), ortho- and para-gneisses, marble, serpentinized harzburgite and garnet-bearing pyroxenite. They constitute ophiolite suites in two cross-sections described below.

3.1. Rock assemblage and petrography

3.1.1. Eclogite

Eclogite in the North Dulan belt occurs as lens-shaped blocks of various-sizes within both granitic and Al-rich pelitic gneisses; some larger ones are very fresh but most have retrogressed during exhumation and fluid alteration. The largest block is up to 300 × 1000 m in size, intercalated in pelitic gneisses in the NDB. The NDB eclogites consist of peak assemblages of Grt + Omp + Rt + Phn + Coe (Qtz pseudomorph) + Zrn + Ap and Grt + Omp + Ep + Ttn + Cal (Arg) + Zrn, and display distinct, retrograde low Jd-content Cpx^{II} + Ab (symplectite) and amphibolite facies assemblages of pargasitic Hbl + Pl + Ep/Czo in some blocks. Most fresh eclogites show granoblastic texture, but the modal content of minerals varies in different blocks. Coesite inclusion and its pseudomorph have been recognized in garnet and omphacite (Song et al., 2003a; G.B. Zhang et al., 2009a,b; J.X. Zhang et al., 2009a,b; J.X. Zhang et al., 2010). Inclusions of K-feldspar (K-cymrite) + Qtz polycrystalline aggregate have also been identified

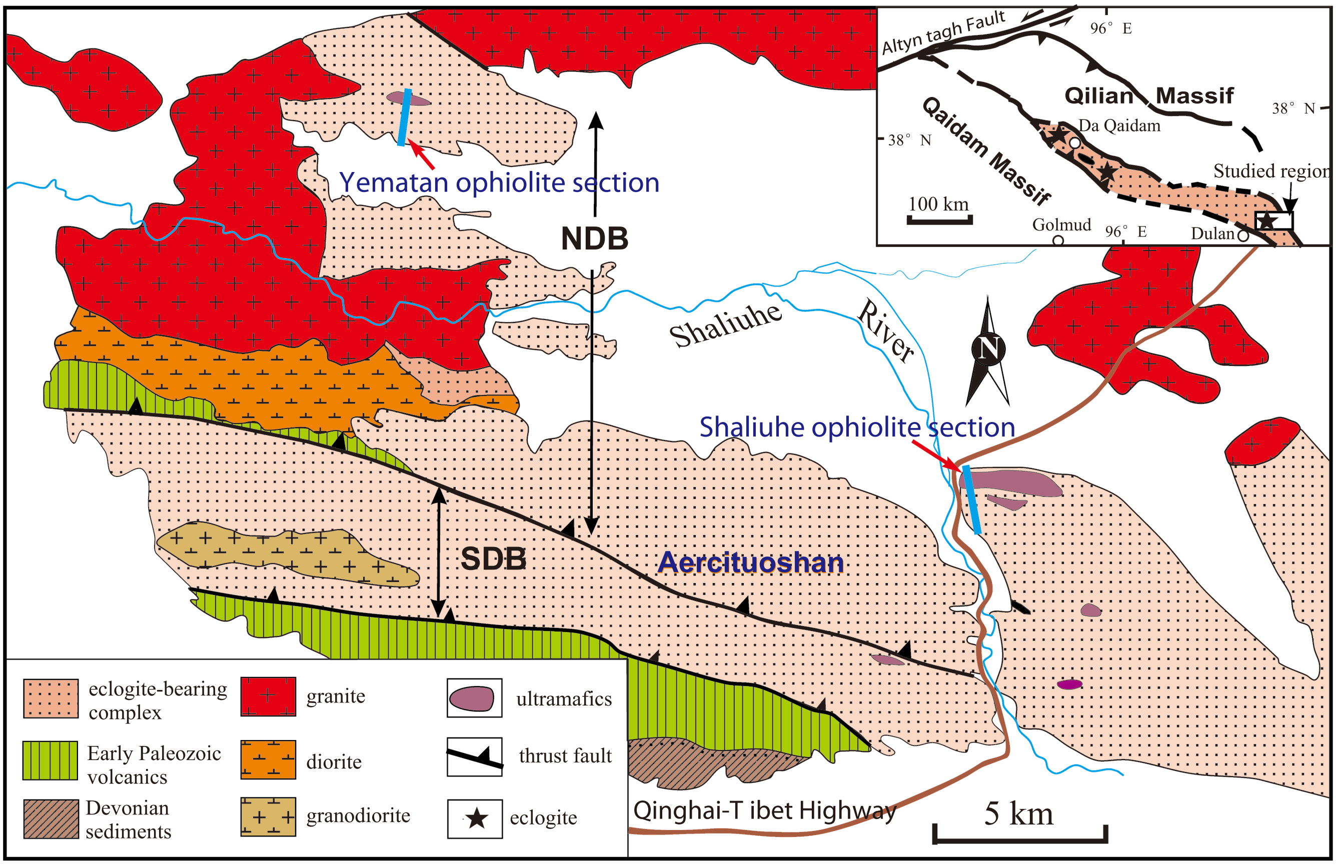

Fig. 3. Geological map of the Dulan UHP terrane (Modified after Song et al., 2003a and Zhang et al., 2010a,b).

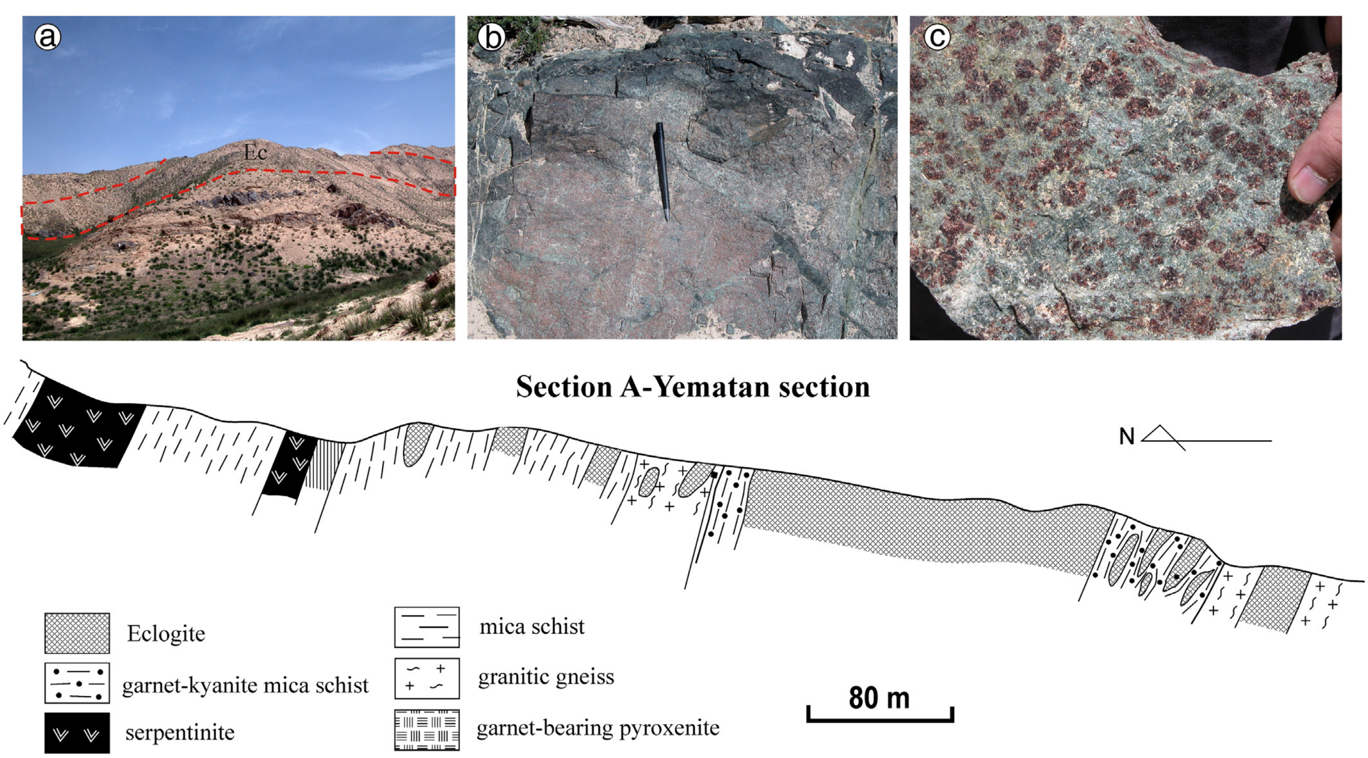

Fig. 4. Yematan cross-sections and field photographs showing fragments of eclogite-facies metamorphic ophiolite sequence. (a) far-view for the cross-section with large blocks of eclogite. (b) eclogite from low-K tholeiite. (c) Ep-eclogite from gabbro.

in Dulan eclogites (Song and Yang, 2001; Song et al., 2003a; R.Y. Zhang et al., 2009).

Protoliths of eclogite blocks are mainly derived from (1) ~820 Ma volcanic rocks (J.X. Zhang et al., 2010) and (2) 540–500 Ma ophiolite (G.B. Zhang et al., 2008).

3.1.2. Pelitic and granitic gneisses

Pelitic gneisses occur as blocks with eclogite intercalated within the granitic gneiss. It usually show strong foliation and consist of garnet (5–8%), biotite (5–10%), muscovite (10–40%) in addition to quartz and sodic plagioclase. Garnet is Alm-rich (up to 80 mol%); kyanite appears in many pelitic gneisses in both sub-belts and is replaced by muscovite. REE-rich allanite also occurs in some pelitic gneiss.

The granitic gneiss is a major rock assemblage and occupies about ~80% of the Dulan eclogite-gneiss UHPM terrane. The gneisses are white to pale gray and show medium- to coarse-grained granoblastic texture with strong foliation. They consist of K-feldspar, plagioclase, quartz, muscovite, and tourmaline, and lack of garnet.

3.1.3. High-pressure granulite and adakitic melts in the SDB

Most SDB eclogites have been overprinted by granulite-facies metamorphism and formed mafic granulite (garnet-clinopyroxenite) (Song et al., 2003a; Yu et al., 2009, 2010). The mafic granulite generally shows homogenous, medium- to coarse-grained granoblastic texture. Based on reaction textures, three main metamorphic stages are recognized: (1) a peak eclogite facies stage identified by Omp (+ rutile) inclusions in Kyanite; (2) a granulite facies stage with development of Grt + Cpx^{II} + Pl ± Scp; and (3) an amphibolite facies stage with Hbl + Czo + Bt + Ab.

Tonalitic and trondhjemitic (adakitic) melts were also reported in association with the high-pressure granulite in the SDB (Song et al., 2009d; Yu et al., 2012; Song et al., in revision).

3.2. UHP metamorphosed ophiolitic sequence in the NBD

3.2.1. Ophiolite-like sequence in Yematan section

An 80-meter-thick garnet-bearing, strongly serpentinized peridotite block occurs with garnet-bearing pyroxenite and eclogite in the Yematan section (Section A, Fig. 4). The garnet pyroxenite was interpreted to be an ultramafic cumulate with high MgO (18.8 wt %), Cr (1095 ppm) and Ni (333 ppm), while eclogite blocks are geochemically similar to present-day N-type to E-type MORB. The rock assemblage most likely represents segments of an oceanic lithosphere (i.e., ophiolitic) from mantle peridotite to Mg-rich cumulate, Ca-rich gabbro, and to basaltic lavas. The peridotite block is strongly serpentinized with relic olivine, Cpx and garnet (Mattinson et al., 2007).

3.2.2. Ophiolite sequence in Shaliuhe Section

Another large ultramafic block (~400 × 800 m in size) has been reported along the Shaliuhe cross-section in the south Dulan belt (G.B. Zhang et al., 2005; J.X. Zhang et al., 2005; G.B. Zhang et al., 2008; J.X. Zhang et al., 2008). Fig. 5 shows three rock types in the northern

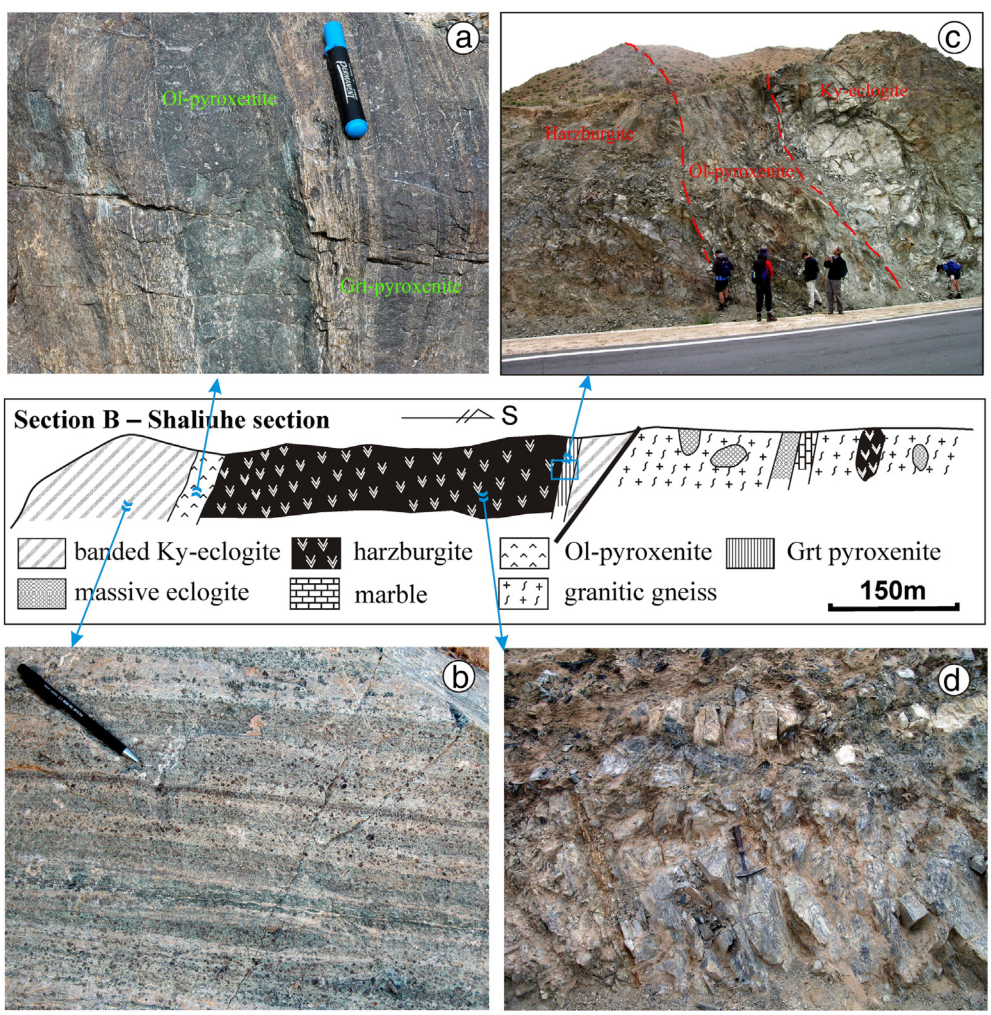

Fig. 5. Shaliuhe cross-sections showing a UHP metamorphosed ophiolite suit. (a) UHP metamorphosed ultramafic cumulate; (b) Ky-eclogite from cumulate gabbro; (c) Field occurrence of serpentinized harzburgite, garnet pyroxenite and banded kyanite (Ky)-eclogite; (d) Serpentinized harzburgite.

part of Section B: (1) kyanite-eclogite, (2) garnet-bearing pyroxenite and olivine pyroxenite and (3) serpentinized harzburgite.

Olivine pyroxenite and garnet-bearing pyroxenite show banded structure (Fig. 5a). The garnet-bearing pyroxenite has retrograded into garnet amphibolite without plagioclase. The olivine pyroxenite shows massive coarse-grained inequireanular, cumulate-like textures with olivine occurring as intercumulus between Cpx grains. These rocks are best interpreted as an Mg-rich cumulate that forms the lower part of an ophiolitic cumulate sequence.

The kyanite-eclogite retains a banded structure that is inherited from original gabbroic cumulate bands (Fig. 5b). The peak metamorphic assemblage is Grt + Omp + Ky + Rt; coesite inclusion and its pseudomorphs were identified in garnet (G.B. Zhang et al., 2009a,b). Geochemical analyses further reveal that this banded kyanite-eclogite has characteristics of cumulate gabbro (or more troctolitic) with high contents of Al_2O_3 (17.2–22.7 wt.%), CaO (12.5–13.5 wt.%), MgO (7.2–13.5 wt.%), Cr (422–790 ppm), Ni (150–254 ppm), low TiO_2 and ΣREE and strong positive Eu and Sr anomalies (G.B. Zhang et al., 2008; J.X. Zhang et al., 2008).

The harzburgite is dark-colored, strongly serpentinized and apparently conformable with kyanite-eclogite and pyroxenites in the cross-section. Relic olivine and opx/opx pseudomorphs were found in some samples.

Two generations of olivine have been recognized in the Shaliuhe peridotite (G.B. Zhang et al., 2005): relict olivine (Ol^1) and metamorphic olivine (Ol^2). The first generation of olivine (Ol^1) occurs as small relict crystals among serpentines, and some crystals retain clear kink-bands with a narrow range of Fo content from 0.88 to 0.91 and relatively high NiO content from 0.28 to 0.46, which is consistent with the olivine compositions from the present-day abyssal peridotite (Dick, 1989). The second generation (Ol^2) occurs as large and dirty crystals with a dense cluster of tiny fluid inclusions. EMP analysis shows these olivines have extremely high Fo content of 0.94–0.97 but low NiO content (0.21–0.35 wt.%), suggesting metamorphic origin through recrystallization of serpentines during continental subduction (e.g., Guillot et al., 2001).

Opx in the Shaliuhe harzburgite occurs as relic crystals surrounded by talc (Tc) + anthophyllite (Ant) corona. High concentrations of Cpx lamellae occur in the relic Opx crystals, suggesting high CaO-content in the original host Opx that should be stable at magmatic conditions (>1100 °C, Lindsley, 1983; Niu, 1999). EMP analysis shows that Opx from the Shaliuhe harzburgite has high Al_2O_3 (2.69–4.63 wt.%) and high and constant $Mg^\#$ (0.91–0.92), which is within the compositional

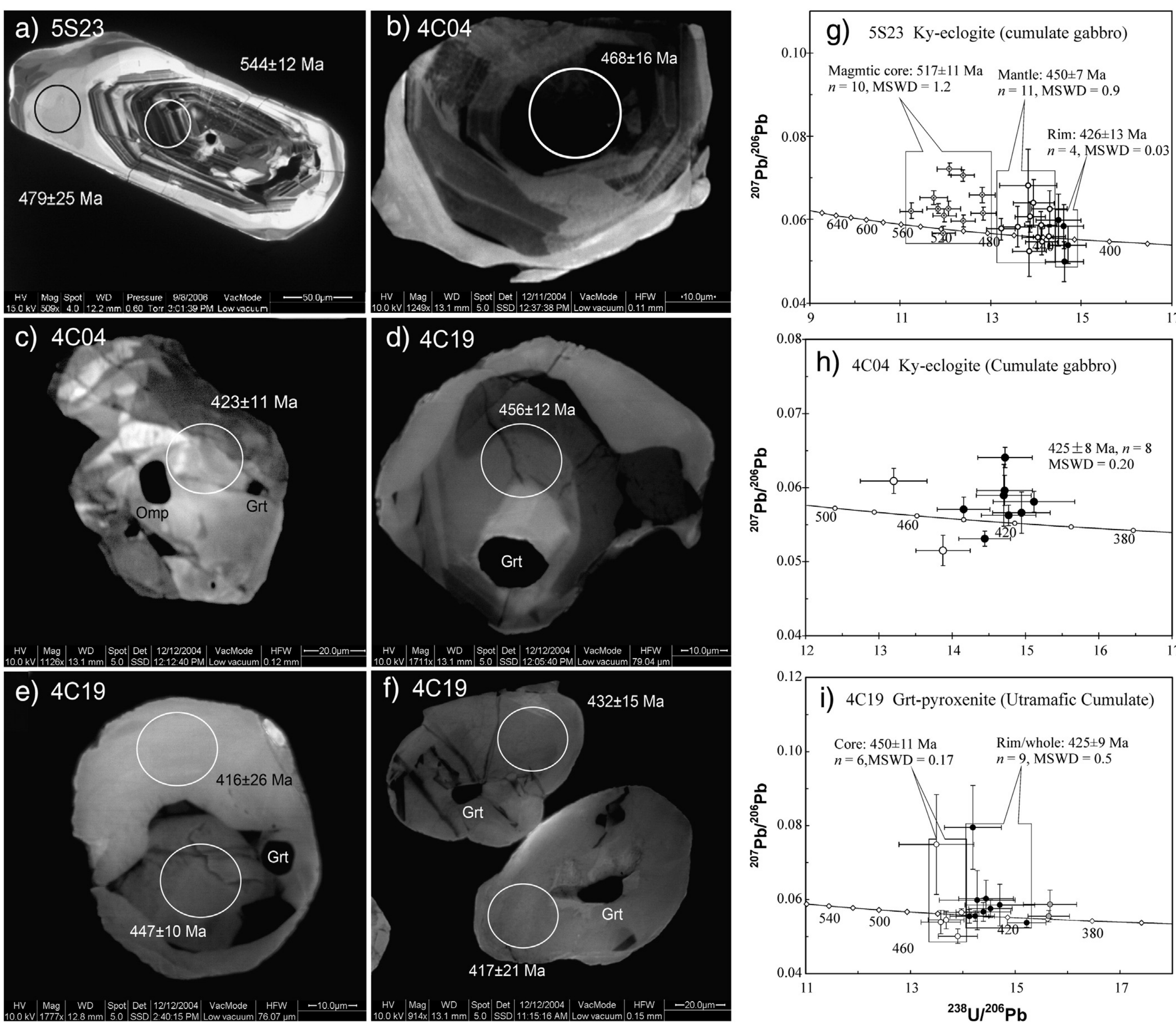

Fig. 6. Zircon CL images (a–e) and Tera–Wasserburg (TW) diagrams for zircons from Shaliuhe meta-cumulates (g–i) (Data of ky-eclogite 5S23 is from G.B. Zhang et al., 2008; J.X. Zhang et al., 2008).

range of Opx from present-day abyssal peridotites, but differs from Opx in the Lüliangshan garnet peridotite.

3.3. Protoliths and metamorphic ages for the Dulan UHP rocks

3.3.1. Protolith and metamorphic ages of the Shaliuhe ophiolite

Three samples, including garnet pyroxenite (banded ultramafic cumulate 4C19) and kyanite eclogite (banded gabbro 5S23 and 4C04), have been selected for zircon U–Pb geochronological analysis. Zircon grains from 5S23 possess well-preserved magmatic cores (Fig. 6a) and yielded $^{206}Pb/^{238}U$ ages of 550–500 Ma with a mean of 517 ± 11 Ma by U–Pb SHRIMP dating (G.B. Zhang et al., 2008), which represent the protolith age of the oceanic crust, similar to ages of ophiolite in the North Qilian suture zone (Song et al., 2013). Fourteen dark-luminescent mantle domains yielded a weighted mean age of 450 ± 7 Ma and 5 zircon rims gave an age of 426 ± 13 Ma (Fig. 6g), which might represent two stages of eclogite-facies metamorphism, respectively. Zircons from 4C04 yielded ages of a mean $^{206}Pb/^{238}U$ age of 425 ± 8 Ma except for two core ages of 470 Ma and 449 Ma (Fig. 6b,c,h). Zircons from the garnet-pyroxenite 4C19 are metamorphic origin with dark-luminescent, “fir-tree” zoned cores and bright-luminescent rims (Fig. 6d,e). Garnet inclusions occur both in the core and in the rim domains (Fig. 6f), suggesting two stages of high/ultrahigh-pressure metamorphism. Five analyses for cores by SHRIMP yielded ages of 447–460 Ma with a weighted mean of 450 ± 11 Ma (MSWD = 0.17), and nine for rim or bright-luminescent grains yielded ages of 438–411 Ma with a mean of 425 ± 9 Ma (MSWD = 0.50) (Fig. 6i).

3.3.2. Metamorphic ages of the NDB pelitic gneisses and eclogite in Yematan

Using CL and SHRIMP technology, Song et al. (2006) determined a peak UHP metamorphic ages 423 ± 6 Ma and a retrograde age of 403 ± 9 Ma for coesite-bearing zircon grains in the NDB pelitic gneiss from the Yematan area. Mattinson et al. (2009) also reported similar metamorphic ages of 426 ± 4 and 430 ± 5 Ma for two metapelite samples. Plotting all zircon analyses (51 spots except for the detrital cores) in the Histograms diagram (Fig. 7), a major peak at 426 Ma and weak peaks at 407 Ma and 398 Ma are obtained, which represent the peak UHP metamorphic age and retrograde age, respectively.

Dating of zircons from the NBD eclogite is more complete than dating of zircons from metapelites. Song et al. (2006) reported a zircon U–Pb mean age of 457 ± 7 Ma (MSWD = 0.91, n = 15) from a fresh eclogite (2D155). This age is consistent with the whole-rock–garnet–omphacite Sm–Nd isochron ages (458 ± 10 Ma and 459 ± 3 Ma, Song et al., 2003b). Eclogitic mineral inclusions, including garnet, omphacite and rutile, suggest that this age represents eclogite-facies metamorphism ~20–30 Myr earlier than coesite-bearing UHP metamorphic ages.

Sample 2D73 is also a very fresh eclogite with granoblastic assemblage of Grt + Omp + Rt from the Yematan area, the north Dulan belt, without amphibole overprinting. Zircon grains recovered from this sample exhibit inner structure with strong luminescent, fir-tree zoned cores and weak luminescent rims of variable wideness (Fig. 8a–d). Eight core analyses by SHRIMP gave $^{206}Pb/^{238}U$ apparent ages of 481–445 Ma with a weight mean of 462 ± 13 Ma (MSWD = 0.41) and 14 analyses for rims and weak luminescent grains gave a weighted mean age of 424 ± 13 Ma (MSWD = 0.12) (Fig. 8e).

Mattinson et al. (2006a) reported zircon SHRIMP ages for three fresh eclogite samples from the Yematan area: one sample gave a mean at 452 ± 4 Ma, the second yielded ages ranging from 418–459 Ma with two age groups of 442 ± 4 Ma and 432.5 ± 5 Ma, and the third gave ages of 415–437 Ma with a mean of 423 ± 4 Ma. Plotting all analyzed data (n = 139) except for magmatic cores in the histograms, two age groups can be distinguished: 473–445 Ma and 434–421 Ma (Fig. 8f).

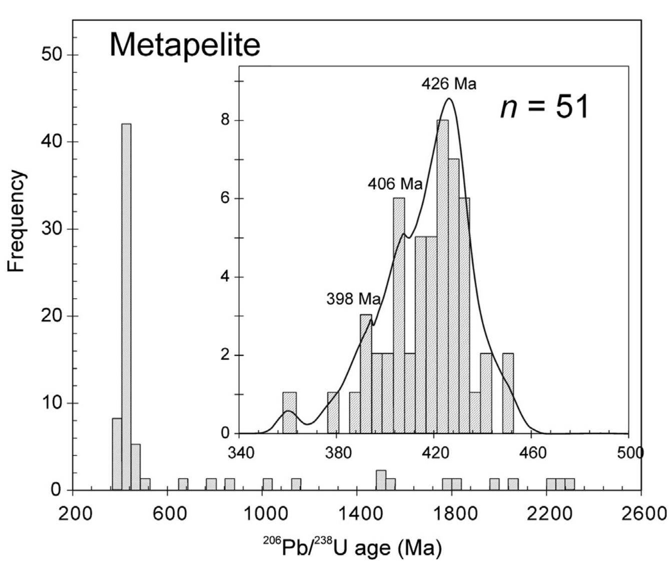

Fig. 7. Histograms of zircon apparent $^{206}Pb/^{238}U$ ages of coesite-bearing paragneiss from Dulan terrane (data from Song et al., 2006; Mattinson et al., 2006a,b, 2009; This study).

3.3.3. Protolith and metamorphic ages of Aerchituoshan coesite-bearing eclogite

J.X. Zhang et al. (2010) documented detailed dating results of zircons from four coesite-bearing eclogite samples in the Aerchituoshan region (see Fig. 3 for location). Coesite-bearing zircons from two samples yielded UHP metamorphic ages of 438 ± 2 Ma and 430 ± 4 Ma. The relic magmatic cores gave protolith age of ~832–838 Ma, similar to eclogite protoliths of Yuka eclogite (Song et al., 2010). Zircons from another sample dating by LA–ICP–MS gave concordant mean ages of 446 ± 3 Ma; these zircons have no relic magmatic cores.

3.3.4. Protolith and metamorphic ages of the granitic gneisses

Four granitic gneiss samples in the Dulan terrane were dated by using zircon U–Pb SHRIMP method. Zircons from granitic sample 07DL73 exhibit clear internal zoning with inherited magmatic cores and metamorphic rims. Five detrital cores yield a weighted mean $^{207}Pb/^{206}Pb$ age of 1566 ± 19 Ma and six rims give a weighted mean $^{206}Pb/^{238}U$ age of 431 ± 4 Ma (MSWD = 1.14). All analyses define a mixing line in the Concordia diagram with an upper-intercept age of 1575 ± 19 Ma and a lower-intercept age of 422 ± 22 Ma (MSWD = 2.1) (Song, unpublished data). The inherited core age should represent the forming time of the granitic protolith, while the rim age is consistent with the UHP metamorphic age by coesite-bearing zircons from meta-pelites.

Zircon grains from the major granitic gneiss show perfect euhedral crystals with the least metamorphic rim. U–Pb analyses for zircons from the granitic gneiss sample (DL31) in the Dulan terrane form an approximately concordant population with a mean $^{207}Pb/^{206}Pb$ age of 907 ± 18 Ma (n = 22, MSWD = 0.36). Zircon grains (n = 28) from the other sample (9Q13) in Dulan terrane form a discordant mixing line with upper intercepts at 936 ± 28 Ma (MSWD = 0.18) and a mean $^{207}Pb/^{206}Pb$ age of 932 ± 18 Ma (MSWD = 0.37) (Song et al., 2012). These ages are consistent with the former zircon SHRIMP dating of 921 ± 7 Ma and 927 ± 7 Ma for two orthogneiss samples by Mattinson et al. (2006b).

3.4. Metamorphic evolution and P–T estimations

Textural relations and mineral paragenesis indicate that eclogites in both sub-belts of the Dulan region experienced multistage metamorphism, but their P–T paths are very different. P–T conditions for peak stage of HP-UHP metamorphism were estimated by geothermobarometers and established phase equilibria.

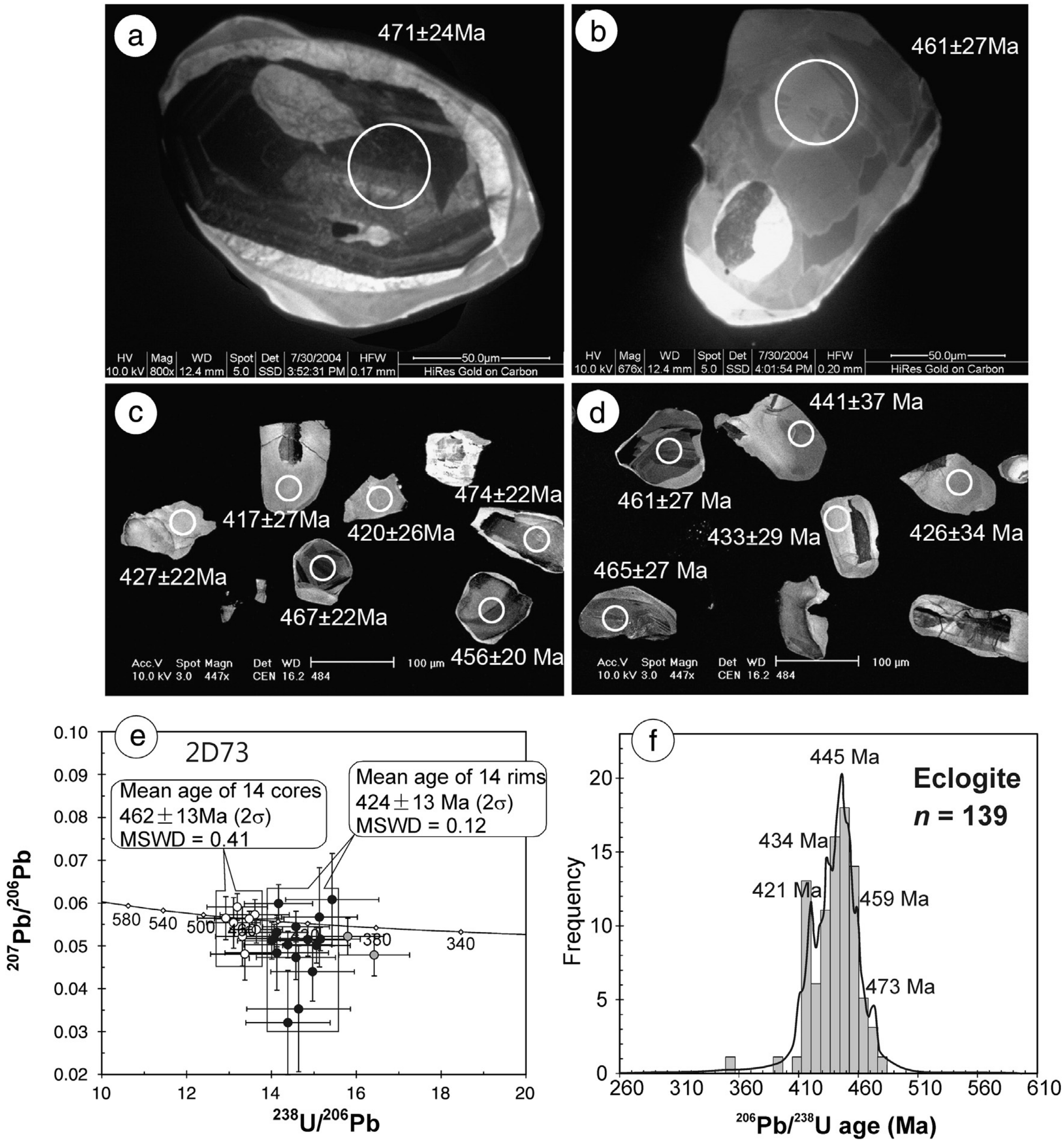

Fig. 8. (a–e) CL images of zircons with age dating spots from eclogite sample 2D73. (e) Tera–Wasserburg (TW) diagrams for zircons from 2D73. (f) Histograms of apparent $^{206}Pb/^{238}U$ age of all analyses of eclogite from Yematan area (data from Mattinson et al., 2006a,b; Song et al., 2006; this study).

3.4.1. P–T conditions of the NDB

Identification of coesite and graphite inclusions in zircon separates from the NDB paragneiss and garnet from the eclogite blocks constrains the pressure limit of peak metamorphism in a range of 2.7–3.5 GPa between the equilibrium curves for the coesite–quartz (Hemingway et al., 1998) and the diamond–graphite (Bundy, 1980) polymorphic transformations (Song et al., 2003a; G.B. Zhang et al., 2008; G.B. Zhang et al., 2009b; G.B. Zhang et al., 2010; J.X. Zhang et al., 2010).

The peak stage assemblages in the NDB eclogites are (1) Grt + Omp + Phe + Rut ± Coe, and (2) Grt + Omp + Ep + Arg. P–T estimates using geothermobarometry of Ravna and Terry (2004) yielded peak metamorphic conditions at T = 630–690 °C and P = 2.9–3.2 GPa. All peak-stage minerals in the NDB eclogites have experienced various degrees of retrograde recrystallization from UHP eclogite to amphibolite-facies conditions. The retrograde reactions include: coesite replaced by quartz, omphacite replaced by Cpx + Ab and further by Hbl + Ab symplectites, garnet and/or omphacite by amphibole and plagioclase, phengite by biotite and plagioclase, and rutile by titanite. The Cpx + Ab vermicular symplectite rims around omphacite also indicate decompression breakdown under 'dry' conditions. The latter assemblage Hbl + Pl + Qtz ± Bi ± Ttn suggests that eclogites were subjected to amphibolite facies metamorphism and constrains P–T conditions around 600 °C and <1.0 GPa.

3.4.2. P–T conditions of the SDB

3.4.2.1. Peak eclogite stage. All eclogite in the SDB are strongly overprinted by granulite facies metamorphism and eclogite-facies minerals, such as omphacite ($Jd_{45–48}$) are preserved as inclusions in kyanite, suggesting similar UHP metamorphic conditions to the NDB eclogite.

3.4.2.2. Granulite overprint stage. Granulite stage metamorphism is characterized by the occurrence of coarse-grained plagioclase, low Jd-content clinopyroxene (Cpx^{II}) and SO_4-bearing scapolite with equilibrium texture. Two Fe^2 + –Mg exchange geothermometers (Powell, 1985; Krogh, 1988) yield temperature in the range 874–948 °C at

2.0 GPa, which are higher than the maximum temperature of the peak eclogite stage. The GADS barometer (An + Di = Grs + Pyr + Qtz) (Eckert et al., 1991) yields concordant results of P = 1.86–1.98 GPa (Song et al., 2003a). Similar P–T results were also reported by Yu et al. (2010). Adakitic magmas occur as melts and a pluton in this sub-belt. They are suggested as melting of thickened lower continental crust (Yu et al., 2012), or decompression melting of the granulitized eclogite during continental subduction and exhumation (Song et al., 2009a,b,c,d, e; Song et al., in revision).

3.4.2.3. Amphibolite facies retrogression stage. Most eclogite and granulite have experienced various degrees of amphibolitization marked by the retrograde assemblage Hbl + Ep/Czo + Pl overprinted on the earlier assemblages at P–T conditions of 0.7–0.9 GPa and 660–695 °C (Song et al., 2003b).

3.4.3. P–T–t paths of the Dulan UHP terrane

Fig. 9 illustrates the P–T–t paths of eclogites and HP granulite from the NBD and SBD. These data allow us to infer that the Dulan terrane in the North Qaidam UHPM belt may have experienced an evolutionary history from oceanic subduction before ~445 Ma to continental subduction to depths >80 km at c. 438–420 Ma and exhumed at c. 420–400 Ma.

4. Xietieshan terrane

The Xitieshan eclogite-bearing terrane is located in the middle part of the Qaidam UHP belt (see Fig. 2 for locality). It is bounded by thrust fault with the Tanjianshan Group, a green-colored, greenschist-facies metamorphosed sequence of volcanic and sedimentary rocks (Cambrian to Ordovician) and famous for lead–zinc deposit (Fig. 10). The Xitieshan terrane mainly consists of felsic gneisses intercalated with varying-sized blocks of eclogite or its retrograde amphibolite, serpentinized peridotite without garnet, and rare marble.

4.1. Eclogite

Eclogites occur as lens-like blocks of varying size, layers and boudinaged dykes within both granitic and pelitic gneisses

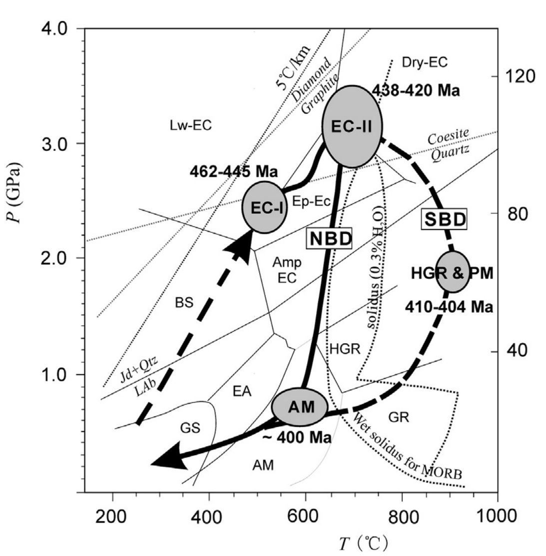

Fig. 9. P–T–t paths of NBD eclogite and SBD HP granulite in the Dulan UHP terrane. P–T boundaries of various metamorphic facies [granulite (GR), high-pressure granulite (HGR), amphibolite (AM), epidote amphibolite (EA), and greenschist (GS)] and subdivision of the eclogite field into amphibole eclogite (Amp-EC), epidote (Ep-EC) eclogite, lawsonite (Lw-EC) eclogite, and dry eclogite are according to Liou et al. (2004). The wet solidi and solidus with 0.3% H2O for middle ocean ridge basalt (MORB) are after Vielzeuf and Schmidt (2001).

(Fig. 10a–d). Some amphibolitized eclogite layers extend for more than 1 km in length. On the basis of mineral assemblage, two types of eclogite can be recognized, i.e., bimineralic eclogite and phengite-eclogite. The bimineralic eclogite is wildly distributed, and strongly retrograde to amphibolites, as black-colored blocks in the field. Only a few fresh eclogite can be preserved in the center of the large block. Phengite eclogite is minor in this area, and also experienced amphibolite overprinting (C. Zhang et al., 2009).

The bimineralic eclogite consists of garnet (35–40%), omphacite (30–40%), amphibole (10–15%) and minor quartz and rutile. Coesite pseudomorph was identified as the inclusion in omphacite (C. Zhang et al., 2009). Phengite eclogite shows coarse-grained, granular texture with the peak assemblage of Grt (30–40%) + Omp (10–15%) + Phn (2–5%) + Qtz + Rt and some blocks are retrograde to garnet–amphibolite. Coesite pseudomorphs in omphacite and coesite inclusions in zircon have been recognized by C. Zhang et al. (2009a) and L. Liu et al. (2012), X.C. Liu et al. (2012a,b), respectively. The peak metamorphic condition of the eclogite was calculated using Grt–Omp–Phn geothermobarometer of Ravna and Terry (2004). Intersection of the Grt–Cpx thermometer and Grt–Phn–Cpx barometer curves yield P = 2.7–3.2 GPa, T = 750–790 °C for the eclogite (C. Zhang et al., 2009).

Although some geochemical data have been published by Yang et al. (2006), origin of eclogite protoliths in the Xitieshan terrane is poorly constrained so far. Some samples have magmatic zircon cores with discordant ages of 750–870 Ma (e.g., J.X. Zhang et al., 2005; Zhang et al., 2006; J.X. Zhang et al., 2009b; C. Zhang et al., 2009; C. Zhang et al., 2011), roughly consistent with the CFBs of Yuka eclogites (D.L. Chen et al., 2009; Song et al., 2010).

4.2. Gneisses

Pelitic gneiss and granitic gneiss occupy more than 80 vol.% of the Xitieshan terrane. Field relationship between pelitic gneiss and granitic gneiss is ambiguous but some researchers suggested the pelitic gneiss was intruded by the orthogneiss (Wan et al., 2006). The pelitic gneiss consists of Grt + Bt + Ky + Pl + Qtz + Rt and kyanite is replaced by sillimenite during decompression (J.X. Zhang et al., 2005; Zhang et al., 2006; J.X. Zhang et al., 2009b; C. Zhang et al., 2009; Zhang et al., 2011). Garnet is compositional zoned with MgO and CaO decrease, and FeO increase from core to rim. Using the compositions of garnet core, plagioclase core and kyanite, the GASP barometry (Grs + 2Ky + Qtz = 3An) yielded pressures of 9.5–11 kbar at 800 °C, and the Grt–Bt thermometry yielded temperature of 719–835 °C at 10 kbar for the pelitic gneiss (J.X. Zhang et al., 2009d). Granitic gneiss consists of K-feldspar + plagioclase + quartz + biotite and lacks evidence of high-pressure metamorphism.

4.3. Geochronology of the Xitieshan HP-UHP rocks

4.3.1. HP-UHP metamorphic ages from eclogite and paragneiss

G.B. Zhang et al. (2005), J.X. Zhang et al. (2005) first reported metamorphic ages of 480 ~ 486 Ma and protolith ages of 750 ~ 800 Ma by zircon U–Pb TIMS and SHRIMP analyses from eclogites in Xitieshan. Ar/Ar ages of amphibole in retrograde eclogites suggest that the eclogites had cooled and exhumed to mid-crustal depths by 407 Ma (J.X. Zhang et al., 2005). J.X. Zhang et al. (2008) obtain the SHRIMP age of eclogite ranging from 426 Ma to 467 Ma, and further divided into two groups. One group with rutile inclusions gives the weighted mean age of 452 ± 12 Ma, which is interpreted as the time of metamorphic zircon growth during HP granulite facies metamorphism. The other group yielded 430 ± 4 Ma and was interpreted as the age of amphibolites facies overprint.

Zircon TIMS dating of an orthogneiss enclosing retrograded eclogite gave an upper intercept of 952 ± 13 Ma and a lower intercept of 478 ± 43 Ma, interpreted as a magmatic crystallization age of the granitic protolith and an early Paleozoic metamorphic age, respectively

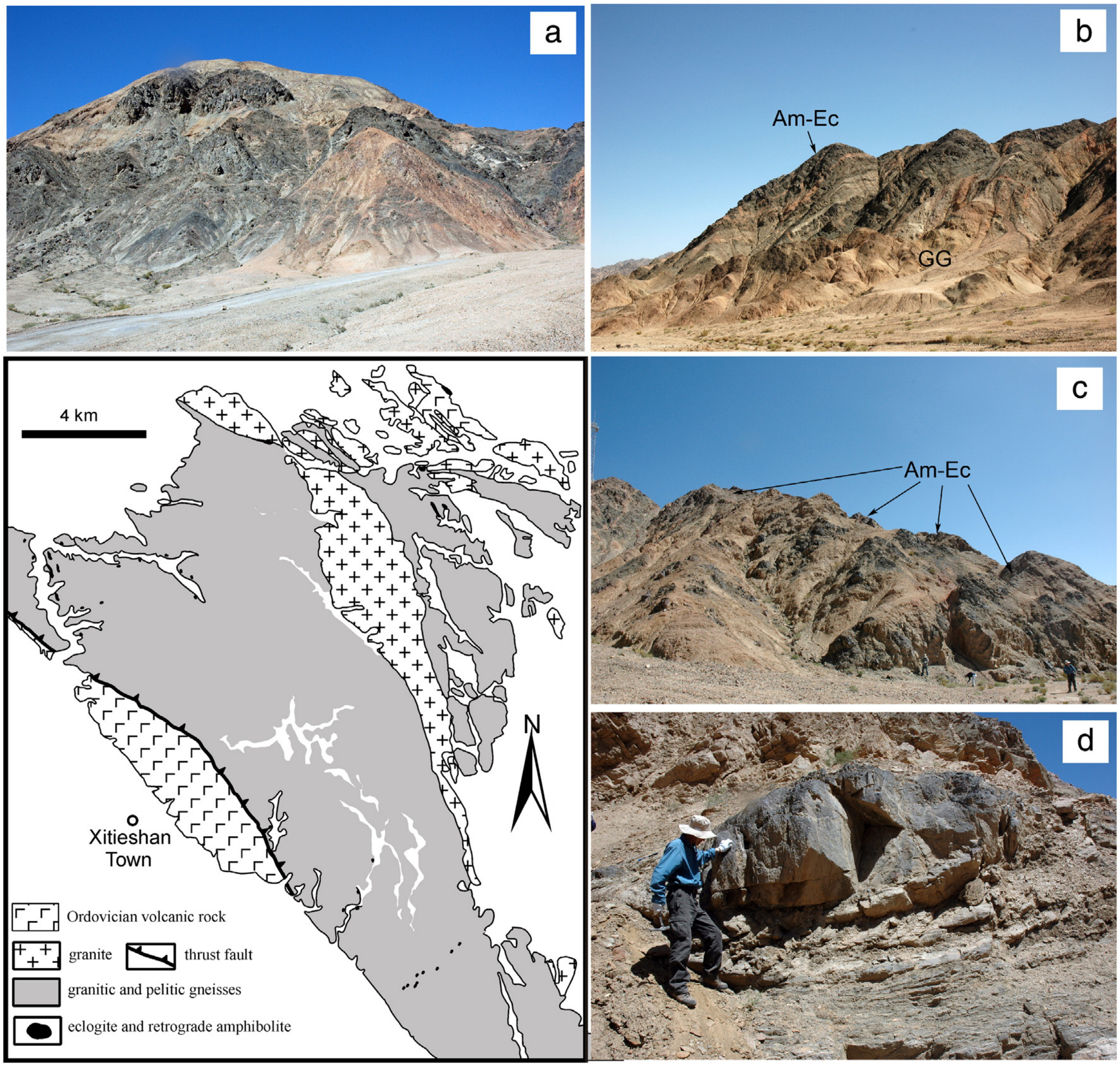

Fig. 10. Geological map (after Zhang et al., 2006) and field photographs of the Xitieshan terrane. (a) Eclogite layer within granitic gneiss. (b)–(c) Amphibolitized eclogite (Am-Ec) layers interbedded with paragneisses. Some eclogite layers extend about 1 km. (d) Lentoid eclogite blocks within the pelitic gneiss.

(Zhang et al., 2006). Zircon SHRIMP dating for garnet-kyanite gneiss records the age of HP metamorphism at 461 Ma, and garnet-sillimanite gneiss also yield the age between 423 and 430 Ma (J.X. Zhang et al., 2008; J.X. Zhang et al., 2009a,b). Therefore, G.B. Zhang et al. (2009a,b), J.X. Zhang et al. (2009a,b), C. Zhang et al. (2009), R.Y. Zhang et al. (2009) interpreted that the high pressure or even ultra-high-pressure metamorphism in the Xitieshan occurs at about 480 Ma and granulite facies overprinting at ca. 450–423 Ma.

However, interpretations by Zhang et al. (2006), J.X. Zhang et al. (2008), and J.X. Zhang et al. (2009b) for these ages are much contradicted with UHP metamorphic ages of eclogite, garnet peridotite and pelitic gneiss from Yuka, Lüliangshan and Dulan terranes. Meanwhile, these ages have not been convinced for which is the eclogite-facies metamorphism. Generally, zircon growth mainly happens in the progression of metamorphism because dehydration reactions can provide enough fluid. From eclogite to granulite facies, on the other hand, decompression with an isograde temperature predominates in solid-transfer reactions, such as Ky = Sill and Omp = Cpx + Ab (symplectite), and these reactions cannot release water. Zircon hardly grows during this stage because neither fluids nor zirconium is provided even in high-grade metamorphic conditions.

More recently, (C. Zhang et al., 2011) reported HP-UHP metamorphic ages of 439 ± 8 Ma and 452 ± 7 Ma (MSWD = 1.8) from two eclogite samples and 422–425 Ma from the garnet-kyanite pelitic gneisses in the Xitieshan terrane, using SHRIMP zircon and monazite EMP (electron microprobe) U–Pb analyses, respectively. Song et al. (2011) also reported a zircon U–Pb age of 432 ± 3 Ma (MSWD = 0.5, n = 15) from an eclogite sample (Q7-15) by a Cameca IMS-1280 ion microprobe. Eclogite-facies mineral inclusions of garnet, omphacite and rutile in these zircons suggest HP-UHP metamorphim.

Plotting all qualified zircon analyses in the histograms, four eclogite samples (J.X. Zhang et al., 2008; Zhang et al., 2011; Song et al., 2011) give two major accumulate age peaks at 435 and 445 Ma and two weak peaks at 405 and 880 Ma (Fig. 11a). The two major age peaks of 435 and 445 Ma should represent two stages of HP-UHP ages of the terrane, similar to the age pattern in the Dulan UHP terrane (see above and the discussion below). The old core age of ~880 Ma was interpreted as magmatic age of protoliths (Zhang et al., 2011), whereas the age of 405 Ma is consistent with retrograde ages in the Dulan UHP terrane (Song et al., 2006). Zircons from 6 metapelitic samples also yield two major accumulate age peaks at 429 and 445 Ma (Fig. 11b), suggesting two stages of HP-UHP metamorphism.

4.3.2. Protolith ages of eclogite and gneisses

As described above, zircons from eclogite preserve relic magmatic cores with ages ranging from 750 to 880 Ma (J.X. Zhang et al., 2005;

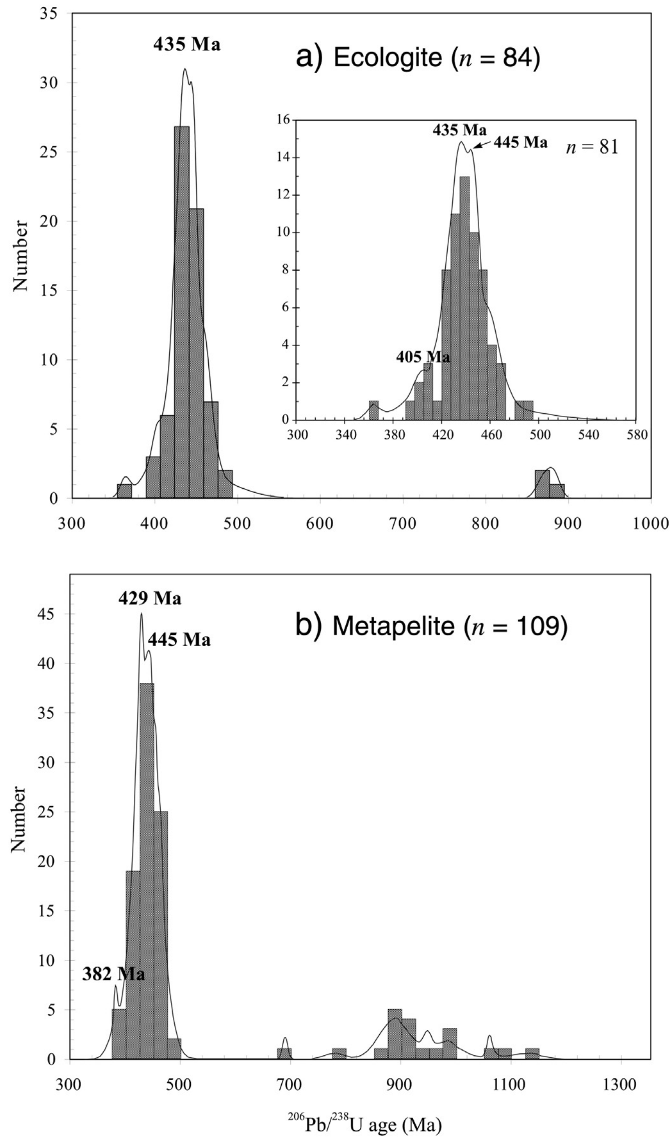

Fig. 11. Histograms of apparent $^{206}Pb/^{238}U$ age of all analyses from (a) four eclogite samples (data from; J.X. Zhang et al., 2008; Zhang et al., 2011; Song et al., 2011) and (b) six metapelite samples (G.B. Zhang et al., 2008; J.X. Zhang et al., 2008; G.B. Zhang et al., 2009a,b; J.X. Zhang et al., 2009a,b; Zhang et al., 2011) in the Xitieshan terrane. Plots generated using ISOPLOT developed by Ludwig (1991).

Zhang et al., 2011), similar to some eclogite protoliths in Dulan (J.X. Zhang et al., 2010) and Yuka terrane (see below). Although their origin has been poorly constrained, the forming ages are consistent with continental flood basalts determined in the Yukan terrane (D.L. Chen et al., 2009; Song et al., 2010).

The granitic gneiss, the major component of the UHPM terrane, is actually the same as those from the Dulan UHPM terrane. Zircon TIMS dating of an orthogneiss by Zhang et al. (2006) gave an upper intercept of 952 ± 13 Ma and a lower intercept of 478 ± 43 Ma. Three granitic samples in this terrane also yielded zircon mean $^{207}Pb/^{206}Pb$ ages of 951 ± 24 Ma (n = 23, MSWD = 0.41) and 942 ± 16 Ma (n = 26, MSWD = 0.42) by LA–ICP–MS (Song et al., 2012). These ages should represent magmatic crystallization age of the granitic protolith.

Most pelitic gneiss samples gave the major Caledonian ages (460–420 Ma, see above) and zircon grains have small detrital cores. Zircons from three samples in the northwest part of the Xitieshan terrane, however, exhibit high-grade (granulite-facies) metamorphic origin with stubby textures of "fir-tree" sector zoning, planar growth banding and radial sector zoning anpboard1d yield Grenvillian ages of 916–952 Ma (Song et al., 2012; C. Zhang et al., 2012). These ages, combining HP-UHP ages of 460–420 Ma for garnet peridotite, eclogite and metapelite published in the literatures (e.g. Song et al., 2005a,b; Mattinson et al., 2006a,b; J.X. Zhang et al., 2006, C. Zhang et al., 2012), suggest that metapelites in the North Qaidam UHP metamorphic belt have experienced two major epochs of metamorphism in Grenvillian and Caledonian, respectively.

5. Yuka eclogite terrane

The Yuka eclogite terrane is located in the northwest end of the North Qaidam UHPM belt (Fig. 2). It extends in NW-SE from Yuka River to the Lüliangshan in the southwest. This terrane mainly consists of various-sized eclogite blocks within para- and ortho-gneisses. Low-grade metamorphosed volcanic rocks (Tuanjianshan group, Cambrain to Ordovician, Wang et al., 2004) are accompanied the Yuka HP-UHP terrane and bounded by thrusting faults (Fig. 12). Eclogite was first reported by Yang et al. (1998). More detailed geochemical and geochronological data have been carried out recently (J.X. Zhang et al., 2004, 2005; Chen et al., 2007a,b; D.L. Chen et al., 2009; G.B. Zhang et al., 2009a; Song et al., 2010).

5.1. Eclogite

Eclogite occurs as layer- or lens-shaped blocks and boudinaged dykes within granitic and pelitic gneisses; some layers are several to tens meters in thickness and extend more than 1 km in length. Most samples are fresh with mineral assemblage of Grt + Omp + Phn + Rt and subsequent lower pressure amphibolite facies overprinting, and show granoblastic texture without shape preferred orientation. Rutile and phengite contents are generally higher than eclogites from Dulan and Xitieshan but the modal content of minerals varies in different blocks. P–T conditions estimated by Grt–Omp–Phn (−Ky) geothermobarometry of Ravna and Terry (2004) are T = 630–730 °C, P = 2.3–2.8 GPa (J.X. Zhang et al., 2005). Recently, a coesite inclusion in garnet has been reported (G.B. Zhang et al., 2009b), which is consistent with the calculated metamorphic P–T conditions.

5.2. Granitic and psammitic/pelitic gneisses

The granitic gneiss is the major component and occupied volume content of ~80% of the UHP terrane. The rocks are off-white colored with mineral assemblage of Pl + Qtz + Ms + minor Kfs. Foliation and isoclinal folds are well-developed in the granitic gneiss. Most granitic gneisses preserve no high-pressure mineral assemblages perhaps due to recrystallization. Rare relic high-pressure inclusions and predicted conditions of garnet growth suggest that the orthogneiss followed a metamorphic P–T path comparable to that of the hosted eclogite with peak pressure at ~2.6 GPa close to the quartz–coesite phase boundary (Menold et al., 2009).

Paragneisses have variable protoliths and compositions, including quartzite (pure sandstone with rare garnet and mica), garnet-mica quartz schist (sandstone with variable pelitic component) and Grt–Ky-mica schist (meta-pelite). They exhibit two field relations with eclogite blocks; some contain lenticular eclogite blocks (Fig. 12a) and some interbed with layered eclogite blocks and granitic gneiss (Fig. 12b). Mineral assemblage in the peltic gneiss is Grt + Phn (Ms) + Qtz ± Pl ± Ky with variable modal contents. No UHP index minerals have been found so far in either matrix or zircon inclusions.

5.3. Ages and geochemistry of the Yuka eclogite

5.3.1. UHP metamorphic ages

HP/UHP metamorphic ages of the Yuka terrane were not determined till recent in situ zircon dating. G.B. Zhang et al. (2005), J.X. Zhang et al.

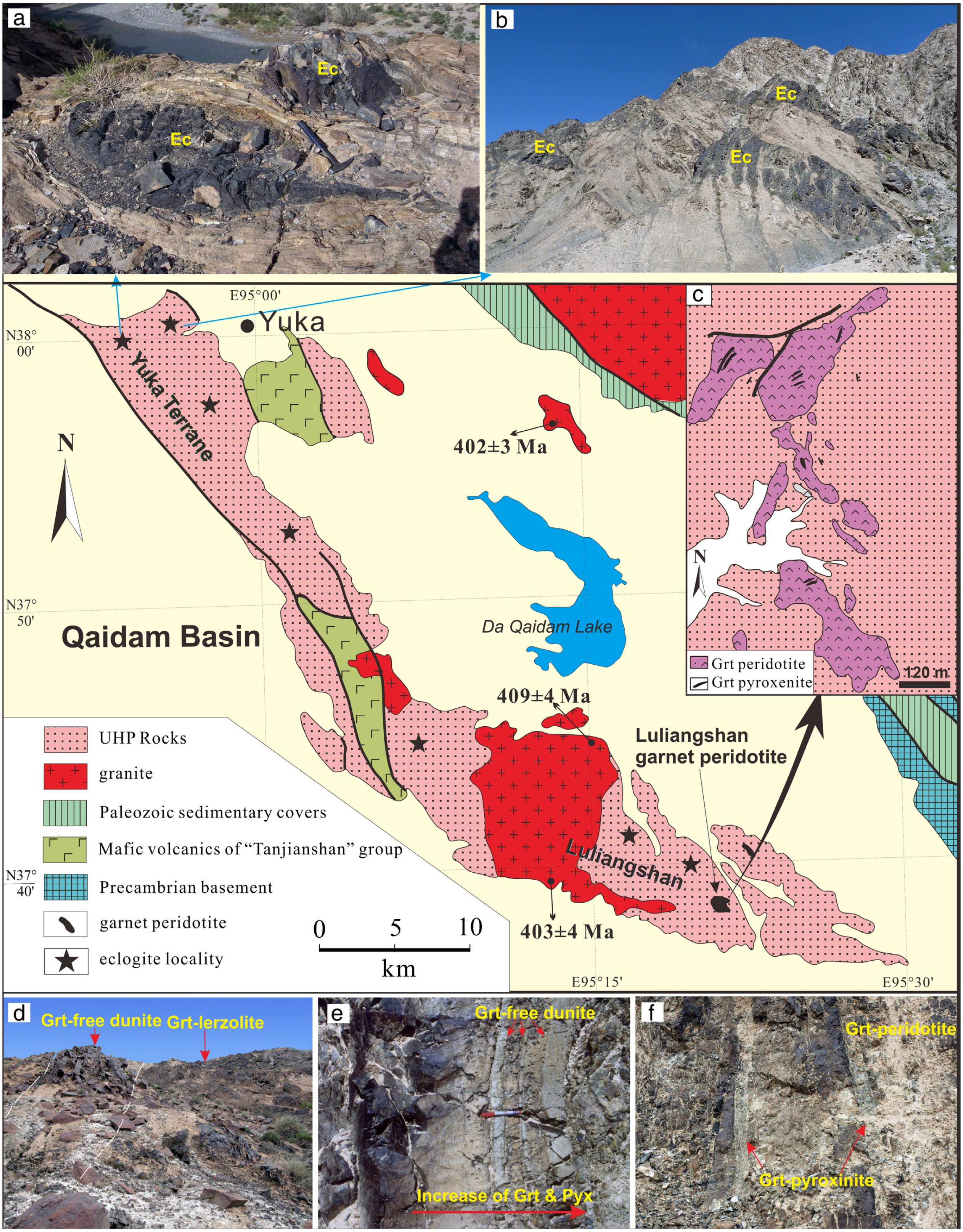
a
Ec
Ec
b
Ec
Ec
Ec
E95°00'
Yuka
N38° 00'
Yuka Terrane
N
402±3 Ma
Da Qaidam Lake
N37° 50'
Qaidam Basin
409±4 Ma
Luliangshan garnet peridotite
Luliangshan
403±4 Ma
N37° 40'
UHP Rocks
granite
Paleozoic sedimentary covers
Mafic volcanics of "Tanjianshan" group
Precambrian basement
garnet peridotite
eclogite locality
0 5 10
km
E95°15'
E95°30'
c
N
Grt peridotite
Grt pyroxenite
120 m
d
Grt-free dunite
Grt-lerzolite
e
Grt-free dunite
Increase of Grt & Pyx
f
Grt-peridotite
Grt-pyroxinite

(2005) reported single zircon TIMS ages of ~500 Ma and phengite Ar–Ar ages of 466–476 Ma, and then they interpreted the former to be the eclogite-facies metamorphic age and the latter to be the amphibolite-facies retrogression. However, CL images show that most zircon crystals from the Yuka eclogite contain inherited magmatic cores and the ~500 Ma TIMS age is most likely a mixing age.

In situ LA–ICP–MS U–Th–Pb analyses of zircons from two eclogite samples gave metamorphic ages of 431 ± 4 Ma to 436 ± 3 Ma with inherited core ages of ~750–800 Ma (D.L. Chen et al., 2009; N.S. Chen et al., 2009). All zircon analyses of eclogite samples in the Histograms diagram (Fig. 13) yield a major peak at 433 Ma and a weak peak at 410 Ma, which represent the peak UHP metamorphic age and retrograde age, respectively. These identical metamorphic ages suggest that the eclogites and host gneisses underwent coeval HP/UHP metamorphism at the same time.

5.3.2. Protolith ages

As mentioned above, most zircon crystals from the Yuka eclogite retain inherited magmatic core; these inherited zircon cores of eclogites have magmatic characters of high REE and HREE abundance, HREE-enriched REE pattern (D.L. Chen et al., 2009; N.S. Chen et al., 2009). Protolith ages of >750 Ma were reported (J.X. Zhang et al., 2008; D.L. Chen et al., 2009; N.S. Chen et al., 2009). Zircons in our two eclogite samples show characteristics that are similar to zircons from mafic volcanic rocks and gave a magmatic crystallization (protolith) age of ~ 850 Ma and a UHPM age of ~ 433 Ma (Song et al., 2010). Given the fact that only limited samples can give a reliable age of high pressure metamorphism in the Yuka eclogite and metapelite samples, we reason that the limited metamorphic growth (thin rims) of zircons suggests a relatively anhydrous condition that frustrated fluid-facilitated diffusion and zircon growth during continental subduction.

5.3.3. Whole-rock chemistry

All Yuka eclogite samples display a relative narrow compositional variation in SiO_2 (43.33–49.47 wt.%), total Fe_2O_3 (Fe_2O_3t, 12.56–16.34 wt.%), MgO (5.3–7.3 wt.%) and Mg-number ($Mg^{\#}$ = 0.55–0.46), but a wide range in $K_2O + Na_2O$ (2.64–4.83 wt.%) and TiO_2 (1.38–4.04 wt.%). On the basis of Ti/Y ratios, the analyzed eclogites can be divided into two major groups: high-Ti group (HTG, Ti/Y > 500, TiO2 > 2.5 wt.%) and low-Ti group (LTG, Ti/Y < 500, TiO2 < 2.5 wt.%). In Nb/Y vs. Zr/Ti diagram (Winchester and Floyd, 1977), all HTG samples plot in the alkaline basalt field, whereas the LTG samples are in the subalkaline basalt field.

The HTG samples have higher abundances of the HFSE and REE ($\sum$REE = 122–199 ppm) and greater light REE enrichment ($[La/Yb]_N$ = 5.22–17.23) than the LTG samples ($\sum$REE = 48–106 ppm; $[La/Yb]_N$ = 1.56–2.95). In general, except for variable LILEs (e.g., Rb, Ba, U and Sr) which could reflect their mobility during seafloor or subduction-zone metamorphism, the HTG samples show "immobile" trace elements characteristics resembling the present-day ocean island basalts (OIB), whereas the LTG samples resemble modern enriched mid-ocean ridge basalts (E-MORB) or transitional type. Nd isotope analyses give $\varepsilon_{Nd\ (t\ =\ 850\ Ma)}$ ranging from −5.34 to +4.47, suggesting variable mantle source or crustal contamination (D.L. Chen et al., 2009; Song et al., 2010). Together with the occurrence and age data, we concluded that the protoliths of the Yuka eclogite are segments of continental flood basalts (CFBs) formed in a rifting setting.

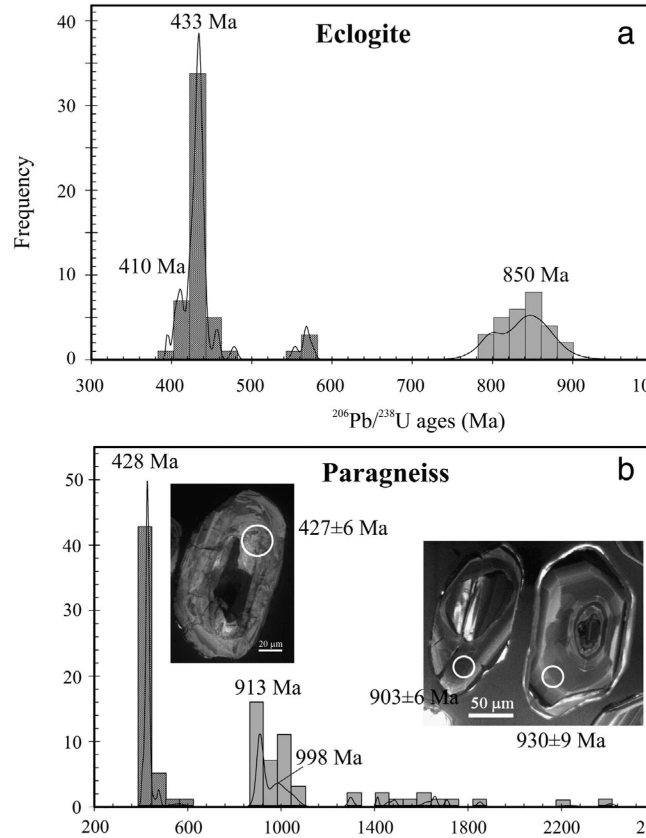

Fig. 13. Histogram of apparent $^{206}Pb/^{238}U$ age of all zircon SHRIMP analyses from Yuka eclogite, North Qaidam UHP belt (data from D.L. Chen et al., 2009; N.S. Chen et al., 2009; Song et al., 2010).

5.4. Protolith of the Yuka eclogite: implications for onset rifting of the Rodinia supercontinent

The protoliths of the eclogites from the Yuka terrane differ significantly from the Dulan ophiolitic sequence (see above). Their occurrence as layers intercalated with terrigenous sedimentary rocks and as dyke-like bodies within the granitic gneisses suggests that the protoliths of these eclogites must be basalts and dolerite dykes from a continental setting. Using Ti/Y ratios, the Yuka eclogite can be divided into two major groups: high-Ti group (HTG, Ti/Y > 500) and low-Ti group (LTG, Ti/Y < 500). In the classification diagram (Winchester and Floyd, 1977), all HTG samples plot in the alkaline basalt field, whereas the LTG samples are in the subalkaline basalt field (Fig. 14a). The high abundances of HFSE and higher Zr/Y and La/Yb ratios are consistent with this interpretation and with their protolith basalts and dolerites being derived from an enriched mantle source. In primitive mantle normalized trace element diagram, the high-Ti and low-Ti groups resemble the present-day OIB and E-type MORB, respectively, suggesting the possibility of their CFB origin (Song et al., 2010). In the La-Y-Nb diagram (Cabanis and Lecolle, 1989) (Fig. 14b), all LTG eclogites plot around the boundary between E-type MORB and continental basalts, and most HTG eclogites fall in the joint regions of continental basalts and alkali basalts from continental rift settings. Therefore, we propose that the

Fig. 12. Geological map and photographs showing field occurrences of various rock types of Yuka eclogite and Lüliangshan garnet peridotite. Zircon ages for granite plutons were reported by Wu et al. (2007). (a) Lenticular eclogite blocks within the metapelite; (b) thick eclogite layers that extend about 1 km interbedded with paragneisses. (c) geological map of the Luliangshan garnet peridotite massif; (d) garnet-free dunite and garnet peridotite; (e) garnet peridotite with 3 layers of garnet-free dunite, note that the rhythmic variation of garnet content in the peridotite layers; (f) garnet pyroxenite interlayers with garnet peridotite.

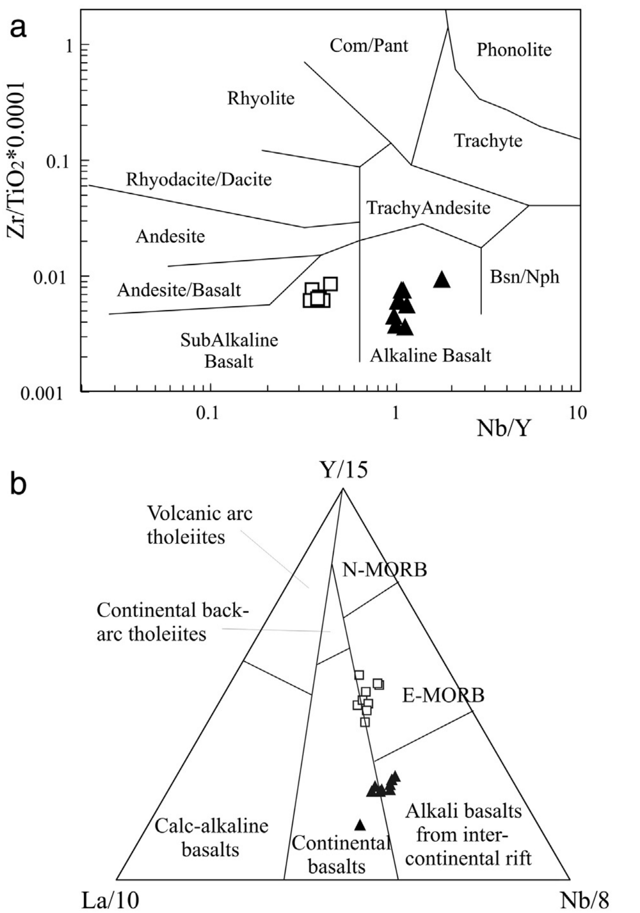

Fig. 14. Diagrams for Yuka eclogites: (a) Classification using Nb/Y vs Zr/Ti (Winchester and Floyd, 1977); (b) La–Y–Nb diagram after Cabanis and Lecolle (1989).

protoliths of the Yuka eclogites are continental flood basalts in its early continental rift stage at ~850 Ma, which may indeed manifest the onset time of large scale magmatic activities within Rodinia.

5.5. Protolith and metamorphic ages of felsic gneisses

5.5.1. Protolith ages of granitic gneiss

All zircon crystals from granitic gneisses show clear oscillatory bands of magmatic origin. U–Pb analysis by using in situ SHRIMP and LA–ICP–MS yielded Grenvillian ages in a range of 900–1000 Ma (Wang et al., 2004; D.L. Chen et al., 2009; Song et al., 2012), the same as protolith ages of granitic gneisses from the Dulan and Xitieshan terranes.

5.5.2. Protolith and metamorphic ages of paragneisses

The layered paragneisses that occur interbedded with the CFB-origin eclogites have age results much different from pelitic gneisses that contain lenticular eclogite blocks. Zircon crystals from the layered paragneiss (mostly psammitic) exhibit complex core-mantle-rim structure in CL images. The cores are detritals of various origin with $^{207}Pb/^{206}Pb$ ages ranging from 2400 Ma to 1300 Ma. The mantles exhibit the type of high-grade metamorphic origin with stubby textures of "fir-tree" sector zoning, planar growth banding and radial sector zoning in CL images (insert photo in Fig. 13b); two samples yield weighted mean $^{207}Pb/^{206}Pb$ ages of 910 ± 10 Ma (Song et al., 2012) and 996 ± 17 Ma (MSWD = 1.7, n = 18) (this study). The rims are very thin (<5 μm) and interpreted as overprinting of UHP metamorphism (Song et al., 2012). These data are consistent with magmatic ages of the granitic gneisses and suggest that the subducted continental crust is predominantly composed of rocks from a Grenville-aged orogenic belt.

Zircons from the pelitic gneiss with eclogite lenses, on the other hand, are uniform and display metamorphic origin with a few detrital cores. D.L. Chen et al. (2009); and N.S. Chen et al. (2009) reported a weight mean age of 431 ± 3 Ma by LA–ICP–MS analysis of zircon from this type of pelitic gneiss. Zircon LA–ICP–MS analyses of our sample (11KL126) in this study also yield a concordant population with a $^{206}Pb/^{238}U$ mean age of 426.5 ± 2.4 Ma (MSWD = 0.02, n = 22). All analyzed data (n = 102 from four samples) plotting in the histograms form two major age groups of 428 Ma and 913–998 Ma (Fig. 13b).

6. Lüliangshan garnet peridotite massif

Garnet peridotite is volumetrically small yet a common component in ultrahigh-pressure (UHP) metamorphic terranes in many continental-type subduction belts. This type of peridotite has received much attention for their special textures, mineral assemblages and ultradeep origin (Medaris and Carswell, 1990; Dobrzhinetskaya et al., 1996; Brueckner, 1998; van Roermund and Drury, 1998, 2001; Brueckner and Medaris, 2000; Song et al., 2004, 2005a,b; Spengler et al., 2006).

The Lüliangshan garnet peridotite massif is a large ultramafic body in the North Qaidam UHPM belt. It was first reported by Yang et al. (1994) and further studied by Song et al. (Song et al., 2004, 2005a,b, 2007a, 2009b,d), Yang and Powell (2008), Shi et al. (2010) and Xiong et al.

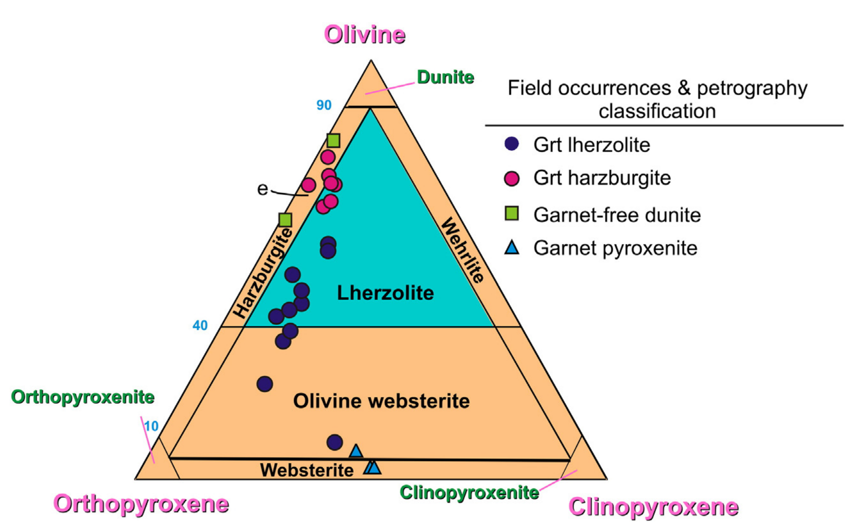

Fig. 15. IUGS rock classification (Streckeisen, 1976) of samples from the Lüliangshan metamorphic garnet peridotite using the protolith mineralogy (after Song et al., 2007a).

(2011). Mineral exsolution lamellae of rutile + two pyroxene + sodic amphibole in garnet and ilmenite + Al-chromite in olivine (Song et al., 2004, 2005a) as well as the presence of a diamond inclusion in a zircon, suggest that this peridotite body experienced ultrahigh-pressure metamorphism at depths in excess of 200 km.

6.1. Occurrence and petrography

The Lüliangshan (also called "Shenglikou" in some literatures) garnet peridotite occurs as a large (~500 × 800 m in size) massif, located in Lüliangshan area, ~20 km south of Da-Qaidam town, and is hosted within an eclogite-bearing quartzofeldspathic gneiss terrane (Fig. 12). This garnet peridotite massif comprises a wide range of lithologies from rocks dominated by olivine to those dominated by pyroxene. On the basis of field and petrographic observations, Song et al. (2005b, 2007a) grouped the rocks into four types: (1) mostly garnet lherzolite with minor amounts of (2) garnet-bearing harzburgite/dunite, (3) garnet-free dunite and (4) garnet pyroxenite dikes/dikelets. Geochemical analyses of these four rock type show a large variation of their bulk-rock compositions: the garnet-free dunite plots in the harzburgite field, the garnet-bearing dunite at the boundary between harzburgite and lherzolite fields, garnet lherzolite in the fields of lherzolite and olivine websterite, and garnet pyroxenite mainly in the websterite field (Fig. 15).

All rock-forming minerals (Ol, Grt, Cpx and Opx) show significantly compositional variation as controlled by whole-rock compositions (Fig. 16). Pyrope composition of garnet increases from 58.8 mol% in lherzolite to 73.5 in garnet harzburgite, and the almandine decreases from 27.1 mol% to 14.7 mol% accordingly (Fig. 16a). Olivine compositions vary in wide range of 83–94 mol% Fo, which is in considerable contrast with olivine compositions of the present-day abyssal peridotite and with sub-continental lithospheric mantle (SCLM) peridotite, but resembles those of ultramafic cumulate complexes (Song et al., 2009d). Orthopyroxene in garnet peridotites shows extremely low in Al_2O_3 (0.3–0.9 wt.%) and a variable X_{Mg} [Mg / (Mg + Fe)] of 0.87–0.96 (Fig. 16c). Clinopyroxene is generally diopside-rich in all rock types with X_{Mg} ranging from 0.92 in the garnet lherzolite to 0.99 in the garnet-bearing harzburgite (Fig. 16d).

6.2. Exsolution lamellae in rock-forming minerals

Decompression-induced exsolution textures are very common in all UHP metamorphic minerals including garnet, olivine and two pyroxenes in garnet-bearing harzburgite, garnet lherzolite and pyroxenite in the Lüliangshan garnet peridotite (Song et al., 2004, 2005a,b). Systematic summary of the exsolution lamellae was given in Fig. 17 by Song et al. (2009d). Exsolutions in olivine from the Lüliangshan garnet peridotite are rods or needles of ilmenite and chromium spinel. Exsolution lamellae in garnets include densely packed rods of rutile, Opx, Cpx and sodic amphibole, suggesting that the inferred majoritic garnet also contains excess Ti, Na and hydroxyl that are only soluble at very high pressures of ≥7 GPa. Clinopyroxene has complex exsolution products in various rock types. Exsolutions in Cpx from garnet dunite and lherzolite include three lamella assemblages: 1) Opx + Cr-magnetite (Cmt), 2) amphibole + Cr-spinel and 3) Opx + amphibole rods/lamellae. The densely packed amphibole and quartz lamellae in

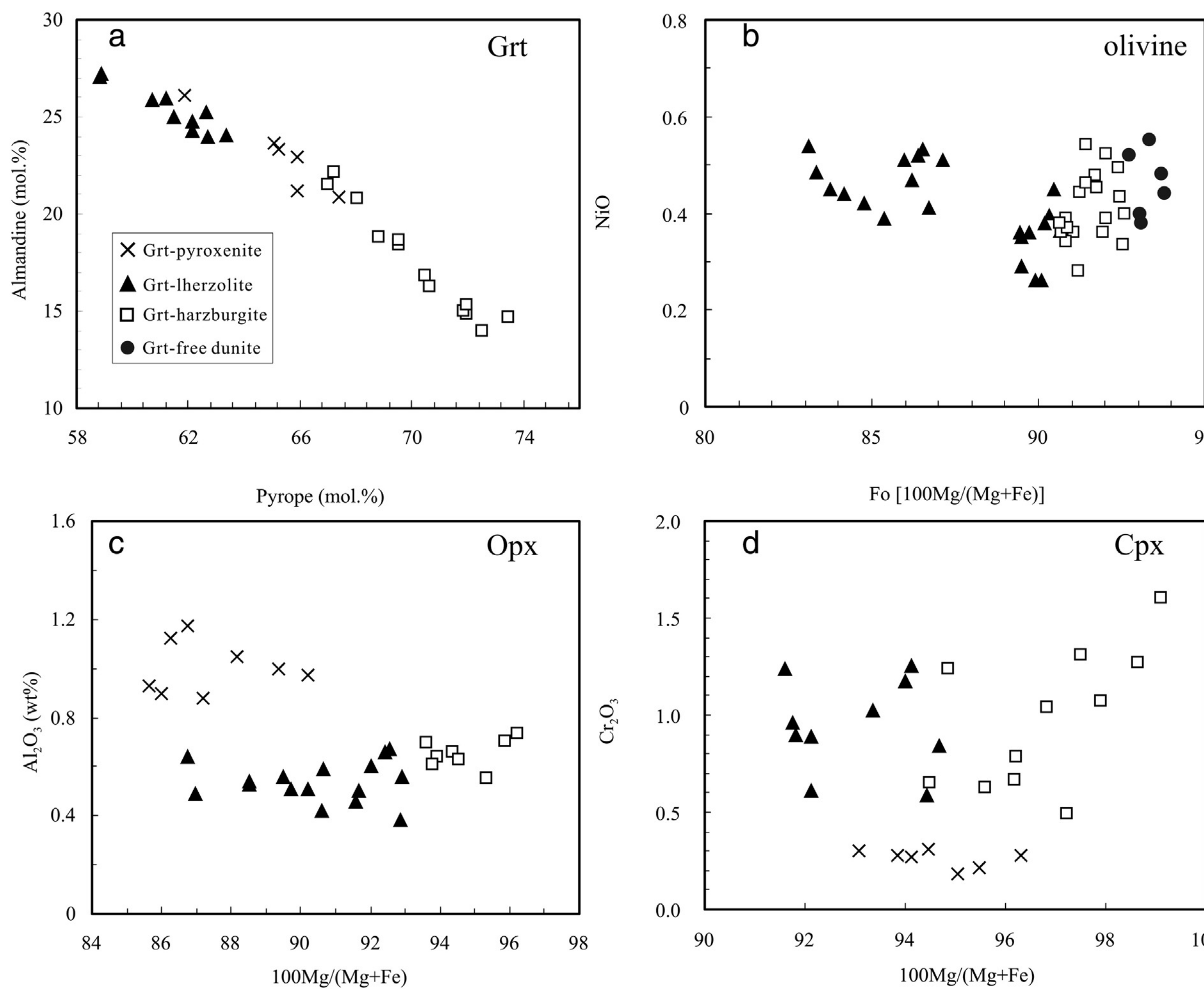

Fig. 16. Compositional variations of major rock-forming minerals of the Lüliangshan garnet peridotite massif.

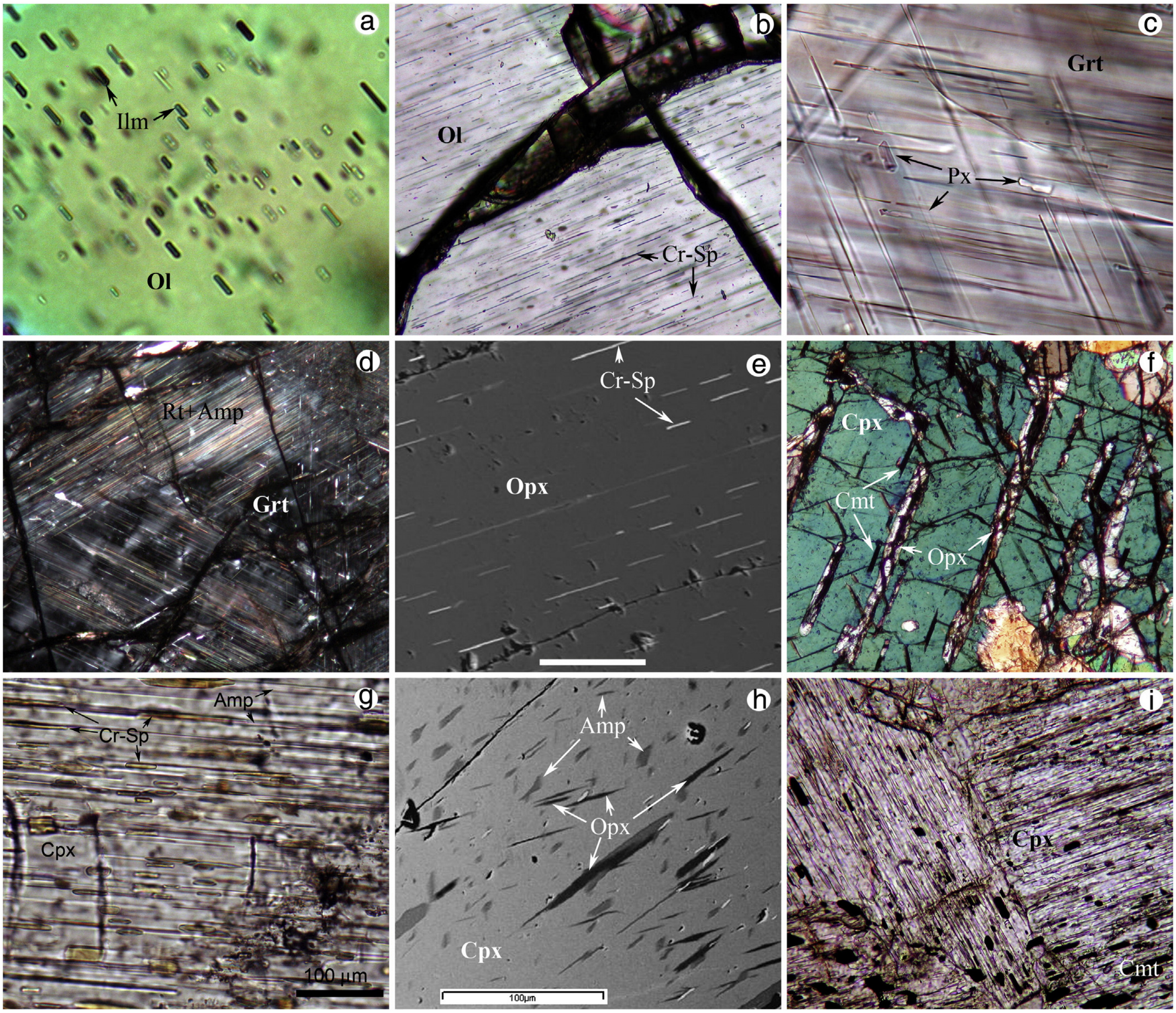

Fig. 17. Exsolution lamellae from major minerals from garnet peridotite and pyroxenite (after Song et al., 2009d). (a) Ilmenite rods in olivine; (b) Cr-spinel needles in olivine; (c) pyroxene lamellae in garnet; (d) rutile + sodic amphibole lamellae in garnet; (e) Cr-spinel needles in opx (BSE image); (f) Opx and Cr-magnetite lamellae in Cpx; (g) Cr-spinel + Amp (+ quartz) lamellae in Cpx; (h) Opx + Amp lamellae in Cpx (BSE image); (i) Amp + quartz + Cr-magnetite lamellae in Cpx.

some Cpx crystals indicate that the parental Cpx was supersilicic and also contained a significant amount of hydroxyl (~2000–3000 ppm).

6.3. UHP metamorphic ages of the garnet peridotite

Song et al. (2005b) reported zircon U–Pb age results by SHRIMP for garnet lherzolite, garnet-bearing harzburgite and garnet pyroxenite Zircons from the garnet lherzolite show four major age groups: (a) 484–444 Ma (weighted mean age, 457 ± 22 Ma) for cores of most crystals, whose morphology and rare earth element (REE) systematics (i.e., very high $[Lu/Sm]_{CN} = 88–230$) suggest a magmatic origin, consistent with the protolith being magmatic cumulate; (b) 435–414 Ma with a mean of 423 ± 5 Ma, which, given by mantle portions of zircon crystals, is interpreted to record the event of ultrahigh-pressure metamorphism (UHPM) at depths greater than 200 km in a continental-type subduction zone; (c) 402–384 Ma (mean age 397 ± 6 Ma) for near-rim portions of zircon crystals. Inherited cores in two zircon crystals were identified using CL and found to be Proterozoic. Morphology and CL images show that are of metamorphic origin. Zircons from garnet-bearing dunite and garnet pyroxenite gave $^{206}Pb/^{238}U$ weighted mean ages of 420 ± 5 Ma and 399 ± 8 Ma, respectively. Recently, Xiong et al. (2011) reported two zircon U–Pb SHRIMP ages of 427 ± 3 Ma and 429 ± 3 Ma, further corroborating that UHP metamorphism of the garnet peridotite happened in the period of 420–430 Ma. All analyses of zircons ($n = 108$) from both garnet peridotite and pyroxenite form a major peak at 426 Ma and weak peak at 401 Ma in the histogram (Fig. 18).

6.4. Protolith of the Lüliangshan peridotite: material from Grenville-age juvenile mantle?

Yang and Powell (2008) interpreted that the Lüliangshan garnet peridotite was formerly mantle peridotite emplaced into the oceanic crust and serpentinized by seawater-derived fluids near the sea floor based on low-temperature mineral inclusions in garnet and olivine. Using Re–Os data and bulk-rock geochemistry, Shi et al. (2010) suggested that the dunites are derived from the Archean (>2.6 Ga) subcontinental lithospheric mantle (SCLM), and the lherzolites were produced

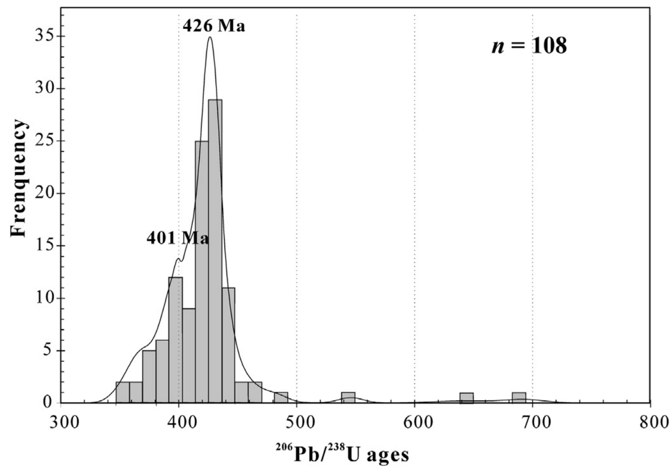

Fig. 18. Histogram of zircon apparent $^{206}Pb/^{238}U$ age of garnet peridotite and pyroxenite from Lüliangshan, North Qaidam UHP belt (data from Song et al., 2005b and Xiong et al., 2011).

though refertilization of dunites by mafic melts (now pyroxenites) during Paleoproterozoic time (ca. 2.2 Ga). Using zircon Hf isotopic data, Xiong et al. (2011) suggested that the Lüliangshan garnet peridotite massif is a fragment from the metasomatized Archean SCLM wedge. However, petrology and mineral compositions do not support the peridotite massif being a fragment of suboceanic or subcontinental lithospheric mantle.

The peridotites show compositional layering that is largely defined by modal variations of major minerals (garnet, olivine, orthopyroxene and clinopyroxene). Rhythmic crystallization bands of the protoliths can be convincingly inferred in some outcrops. These textural observations, together with relic accumulate textures in garnet lherzolite, the large compositional variation of major rock-forming minerals, the documented major and trace element systematics, as well as magmatic zircon cores, strongly suggest that the Lüliangshan garnet peridotite ultramafic cumulate complex crystallized from high-Mg melts in an arc environment before UHP metamorphism. Normative igneous assemblages calculated from the bulk-rock major element compositions (Niu, 1997) vary from harzburgite to lherzolite, and to olivine websterite consistent with increasing bulk-rock Al_2O_3 (also modal garnet) and decreasing bulk-rock MgO (also modal olivine) during crystallization (see Fig. 12 of Song et al., 2007a).

The bulk-rock trace element systematics is consistent with the protoliths being in equilibrium with subduction-zone melts (see Fig. 11 of Song et al., 2007a) or being contaminated by continental crust material in their petrogenesis. Their enriched isotopic compositions (e.g., Nd(t) $< -6.8 \sim -0.5$) and high enrichment in incompatible elements (Song et al., 2007a) indeed suggest that a continental crust component has been incorporated in their parental melts either in the form of (subducted) terrigeneous sediments or from crustal contamination. The accumulated and documented large volume of complementary data and observations is overwhelming evidence that the Lüliangshan garnet peridotite originates from a late Precambrian Alaskan-type ultramafic intrusion (Song et al., 2009d).

Expectedly, zircon Hf isotopic data by Xiong et al. (2011) gave a good constraint for origin of the Luliangshan garnet peridotite. The εHf(t = 427 Ma) value (+2.2 to −2.3) and a small range in T_{DM} (1.12–0.95 Ga) of zircons from the garnet peridotite and pyroxenite (Xiong et al., 2011) lend convincing support for their deriving (partial melting) from a juvenile mantle wedge associated with Grenville-age orogenesis.

7. Post-collisional magmatic sequences

Granitic rocks can be generated in the various stages, e.g., the pre-, syn- and post-collision of the orogeny, and thus are the key to understanding history of plate subduction and exhumation. Besides adakitic rocks in the Dulan UHPM terrane that were interpreted either as decompression melting of eclogite during continental subduction and exhumation, or as crustal thickening during continental collision (see above), a zone of diorite–granodiorite–granite plutons intrudes UHP metamorphic rocks between the north and south Dulan belts (Fig. 3). These plutons show homogeneous medium to coarse-grained granitic texture without any deformation. Rock assemblage includes amphibole diorite, tonalite, granodiorite and monzonitic granite, similar to magmatic assemblage in the active continental margin. Geochronology studies for zircon from a granodiorite gave a weighted mean age of 397 ± 3 Ma (Wu et al., 2004; Yu et al., 2012). Zircons from monzonitic granite and diorite samples yielded zircon LA–ICP–MS ages from 384 to 360 Ma (Wang and Song, in preparation).

From Yuka to Xitieshan, a number of granitic plutons of post-collisional granite plutons that intrude in the UHP rocks and postdate the UHP metamorphic ages were also recognized in two stages at 409–403 Ma and 375–370 Ma (Wu et al., 2007) (see Figs. 10 and 12). Some granites exhibit adakitic affinity with high Sr (424–1006 ppm), low Y (3.7–14.4 ppm), high Na_2O/K_2O (1.5–4) and La/Yb ratios, whereas the other granites show red color in the field and S-type in composition with high K_2O (3.3–5.1 wt.%), low Sr (102–237 ppm) and pronounced Eu negative anomaly (Eu/Eu* = 0.35–0.58).

These age data indicate that the post-collisional magmatic activity started ~10–20 Myr later than the UHPM time and continued ~40 Myr during extension and mountain collapse.

8. Discussion

8.1. UHPM protoliths of the subducted complex: records of Grenville orogenesis, Neoproterozoic CFBs and Early Paleozoic ocean crust

As a continental-type subduction belt, in general, the components in the North Qaidam UHPM belt are predominantly materials from a continental crust, which resemble features of typical continental-type UHP terranes such as Dabie-Sulu in Eastern China and the Western Gneiss Region in Norway (Liou et al., 2009). Rock assemblage in such kind of UHPM belt consists of granitic gneiss, medium to high temperature eclogite, metapelite and marble, and garnet peridotite, which differs from rocks in the oceanic-type subduction belts (ophiolitic mélange, arc volcanic rocks, and HP/LT blueschist and eclogite) (e.g., Song et al., 2006). These continental components might be inevitably mixed with sediments from the continental margin, even with some fragments of oceanic crust.

Hf isotopic data reflect a large extent of initial heterogeneity for both zircons from eclogite blocks ($\varepsilon_{Hf}(t) = +14.0$ to -19.5) and zircons from felsic gneisses ($\varepsilon_{Hf}(t) = +15.8$ to -17.9; crustal model ages from 2.54 Ga to 0.80 Ga), which were interpreted as the protoliths of the UHPM rocks being formed by magmatic mixing between juvenile components from the depleted mantle (DM) and evolved material from the Archean Qaidam crust (Xiong et al., 2012).

8.1.1. Granitic gneiss—products of the Grenville-age orogeny

In the North Qaidam UHP belt, granitic gneiss is the major component that occupies more than 80 vol.% of the whole UHPM belt. It hosts or interbeds with relatively minor eclogite, peridotite and metapelite blocks. All these granitic gneisses are deformed or mylonized with penetrated foliation. Most granitic gneisses preserve no high-pressure assemblage, which might be partially explained by the facility of recrystallization in felsic rocks.

The forming ages of the granitic gneiss in the three major terranes of the North Qaidam UHPM belt concentrate in a narrow range from 900 Ma to 1020 Ma (Song and Yang, 2001; Lu, 2002; D.L. Chen et al., 2009; N.S. Chen et al., 2009; G.B. Zhang et al., 2009a,b; Song et al., 2012), except for one gneiss sample from Dulan terrane with a protolith age of 1566 ± 19 Ma in this study. No Paleoproterozoic rocks have been found in the whole UHPM belt. This suggests that the subducted continental crust is a juvenile crust that was associated with Grenville-age orogeny, similar to the Sibao orogenic belt between the Yangtze and Cathaysia blocks (e.g., Li et al., 2008), and can be interpreted as a Grenvillian suture that assembled the supercontinent Rodinia at ~900–1000 Ma. However, detailed work on rock types, geochemistry and petrogenesis of the granitic gneiss remains to be done.

8.1.2. Eclogite protoliths—Neoproterozoic CFBs vs. fragments of Early Paleozoic ocean crust

As described above, magmatic zircon cores in most eclogite blocks in the Yuka terrane are well preserved and yielded qualified protolith ages of ~850 Ma, suggesting eclogite-facies metamorphism (T = 630–730 °C and P = 2.3–2.8 GPa) at relative "dry" condition. Field occurrence and geochemical features demonstrate that the Yuka eclogite blocks are fragments of CFBs from a continental rifting that broke up the Rodinia. Similar protolith ages (750 Ma to 870 Ma) were also reported in eclogites from Xitieshan and Dulan terranes (J.X. Zhang et al., 2005; J.X. Zhang et al., 2010; Zhang et al., 2011) suggesting CFBs were involved in the whole UHPM belt, although these protolith ages are not as well constrained as the Yuka eclogite. Together with the major component of Grenville-age granites, we can conclude that the subducted slab was derived from a juvenile crust that was formed by multiple continental movements from convergency to divergency in the Neoproterozoic time.

In the Yematan and Shaliuhe sections of Dulan terrane, on the other hand, mantle harzburgite, banded ultramafic to gabbroic cumulates (including olivine-pyroxenite, garnet pyroxenite and kyanite-eclogite) and eclogite of MORB protolith composes typical ophiolite sequences. They represent oceanic lithosphere and have experienced UHP metamorphism at P = 2.9–3.3 GPa and T = 630–720 °C (Song et al., 2003a,b; G.B. Zhang et al., 2008; G.B. Zhang et al., 2009a,b; Song et al., 2009b). These UHP metamorphosed ophiolitic fragments demonstrate that a previous oceanic lithosphere existed in Cambrian or earlier and totally consumed prior to the continental collision. The protolith ages of 500–540 Ma from a gabbroic kyanite-eclogite (G.B. Zhang et al., 2008; J.X. Zhang et al., 2008) are close to the HP/UHP ages (460–420 Ma) of eclogites. Old (600–700 Ma) oceanic fragments might also exist in this belt but have not yet recognized so far. Therefore, the Qilian Ocean must have developed in a long time since the breakup of Rodinia, although the size and detailed history of this ocean are unknown.

8.1.3. UHP pelitic/psammitic gneiss—sediments at a foredeep vs. old paragneisses from the Grenville-age continental crust

Meta-sediment rocks are characterized by high contents of aluminous minerals such as garnet, kyanite and mica and high quartz/feldspar ratios that are distinguished from granitic gneisses. Detrital cores of zircons from meta-sedimentary rocks are well preserved in Yuka terrane and less in Xitieshan and Dulan terranes. The least discordant inherited core ages range from 0.8 Ga to 2.5 Ga and mainly group at 0.8–1.0 Ga, 1.5–1.8 Ga with minor ages of 2.2–2.5 Ga (Song et al., 2006; D.L. Chen et al., 2009; N.S. Chen et al., 2009; Mattinson et al., 2007, 2009; G.B. Zhang et al., 2008; J.X. Zhang et al., 2008), indicating that these sedimentary rocks might deposit at a continental margin that received sediments from both the Grenvillian orogen and the Proterozoic to Archean craton. Therefore, the subducted continental terrane in the North Qaidam UHPM belt shares a common Precambrian history with the Yangtze Craton (e.g., Song et al., 2006; Wan et al., 2006).

Two types of distinct metapelites can be subdivided in all the three UHPM terranes of the North Qaidam UHP belt. Type I metapelites are derived from sediments of foredeep in the subduction zone (e.g. Doglioni, 1994). These rocks were located in front (snout, vanguard) of the subducted continental crust and can seize some fragments of ocean crust (e.g. eclogitized ophiolite blocks in Dulan terrane). Coesite-bearing zircons in such metapelites contain very little detrital core and yield excellent metamorphic ages of ~420–435 Ma (Mattinson et al., 2006a,b; Song et al., 2006 and this study), suggesting that they experienced crystallization with sufficient fluids at UHP conditions. Type II metapelites are derived from continental crust that were formed by high-grade metamorphism during Grenvillian-age orogenesis together with 910–1000 Ma granitic gneisses. They are intercalated with eclogites of ~850 Ma CFBs. Zircons from such metapelites in Xitieshan and Yuka terrane, on the other hand, preserve all information for Grenvillian-age metamorphism with the least Caledonian-age overgrowth (C. Zhang et al., 2012; Song et al., 2012), suggesting an extreme dry condition of a juvenile continent crust.

8.1.4. Two kinds of peridotite blocks—oceanic vs. continental lithospheric mantle

The observation that the orogenic garnet peridotite is exclusively associated with zones of continental collision, but is absent in zones of oceanic lithosphere subduction, has previously suggested a genetic affinity with continental subduction and subsequent continental collision. Petrology and geochemistry revealed that this garnet peridotite might be ultramafic cumulates from a high-Mg magma in the sub-arc environment and subducted with continental crust to ~200 km by corner flow (Song et al., 2007a, 2009d). In contrast, garnet-free, strongly serpentinized peridotite is commonly believed to be restricted to oceanic-type subduction zones and is believed to represent the fragment of oceanic lithospheric mantle (G.B. Zhang et al., 2005; G.B. Zhang et al., 2008; Song et al., 2009b).

All samples of the Lüliangshan garnet peridotite massif yield negative $\varepsilon_{Nd}(t = 460\ Ma)$ values ranging from −0.5 to −6.8 (Song et al., 2007a), which differ from sub-continental lithospheric mantle (e.g., Downes, 2001) and the depleted oceanic lithospheric mantle (e.g., Hart, 1988). The Zircon Hf model ages of 1.12–0.95 Ga by Xiong et al. (2011) suggest that they derived from a juvenile or sub-arc mantle environment associated with Grenville-age orogenesis.

8.2. Time constraint for oceanic subduction, continental subduction and exhumation

8.2.1. Determination of UHP metamorphic time for continental subduction

Rock assemblages and presence of index minerals (e.g., coesite and diamond) indicate that the North Qaidam is a typical UHPM belt that resulted from continental-type subduction, similar to UHP terranes of Dabie-Sulu in Eastern China and WGR in Norway. As shown in Table 2 (single zircon TIMS ages are excluded), a large number of qualified zircon U–Pb ages have been carried out in recent years. In Yuka terrane, eclogite and metapelite have identical zircon ages in a narrow range from 430 Ma to 435 Ma, and imply that they metamorphosed simultaneously during continental subduction to the depths of ~70–90 km (2.3–2.8 GPa). In the Lüliangshan region, zircons from four garnet peridotite samples give UHP metamorphic ages of 420–429 Ma at depths of ~200 km (Song et al., 2005a; Xiong et al., 2011). These ages are consistent with zircon weighted mean age of 424 ± 4 Ma from a grt–ky–mica schist (Ma and Chen, 2006) and 421 ± 5 Ma from a retrograde (symplectized) eclogite (Zhang et al., 2007b). In Xitieshan terrane, eclogite-facies metamorphism occurred in a weighted mean age of 433 ± 3 Ma (Song et al., 2011), the same as the Yuka eclogite. In Dulan terrane, two eclogite samples gave zircon (coesite-bearing) SHRIMP weighted mean ages of 430 ± 3 and 438 ± 3 Ma (G.B. Zhang et al., 2010; J.X. Zhang et al., 2010), coesite-bearing zircons from two meta-pelitic samples yielded ages of 423 ± 6 Ma (Song et al., 2006) and 426 ± 3 Ma (this study), consistent with weighted mean ages of 426 ± 4 Ma and 431 ± 5 Ma reported by Mattinson et al. (2009). Mineral inclusions such as coesite, diamond, garnet and phengite in zircons demonstrate significant growth during UHP metamorphism with high flux of fluid activity. These UHP metamorphic ages recorded by zircons indicate that continental subduction might start at ~438 Ma and continue to ~420 Ma at depths from 70 km to 200 km.

Table 2
Summary on reliable ages of eclogite, felsic gneiss and garnet peridotite in the North Qaidam UHPM belt. Eclogite-facies metamorphic ages can be subdivided into two groups. The bold age numbers are all < 400 Ma and refer to UHPM ages during the subsequent continental subduction.

Rock type	Protolith age (Ma)	HP/UHP age (Ma)	Retrograde age (Ma)	Method	Reference
Yematan and Aerchituoshan, Dulan terrane					
Eclogite	–	459 ± 2.6		Sm-Nd	Song et al., 2003b
		458 ± 10			
Eclogite	–	457 ± 7		SHRIMP	Song et al., 2006
		~426 (1 rim)			
Eclogite	–	449 ± 2		SHRIMP	Mattinson et al., 2006a
Eclogite		442 ± 7			
Eclogite		**433 ± 5**			
Eclogite		**422 ± 4**			
Coe-eclogite	~835	**430 ± 3**		SHRIMP	G.B. Zhang et al., 2010; J.X. Zhang et al., 2010
		438 ± 3		SHRIMP	
	809–820	**430 ± 7**[a]		LA–ICP–MS	
	?	446 ± 3		LA–ICP–MS	
Eclogite	~500	462 ± 13	380–400	SHRIMP	This study
		424 ± 13			
Coe–Grt–Ky schist		**423 ± 6**	403 ± 7 Ma	SHRIMP	Song et al., 2006
Grt–Ky schist		**426 ± 4**		SHRIMP	Mattinson et al., 2009
		430 ± 5			
Granitic gneiss	1566 ± 19	**431 ± 4**		SHRIMP	This study
Granitic gneiss	930–1020			LA–ICP–MS	Mattinson et al., 2006b
			402 ± 2	$^{39}Ar–^{40}Ar$	Song et al., 2006, 2012
UHP meta-ophiolite in Shaliuhe, Dulan terrane					
Ky-eclogite (cumulate gabbro)	500–544	454 ± 12		SHRIMP	G.B. Zhang et al., 2008; J.X. Zhang et al., 2008
	(517 ± 22)	**426 ± 13**			
Ky-eclogite		**425 ± 8**		SHRIMP	This study
Grt-pyroxenite (ultramafic cumulate)		450 ± 11		SHRIMP	This study
		425 ± 9			
Xitieshan terrane					
Eclogite	~ 870	**439 ± 8**		SHRIMP	Zhang et al., 2011
Eclogite	?	452 ± 7			
Eclogite		**433 ± 3**		SIMS	Song et al., 2011
Eclogite		454 ± 6		SHRIMP	J.X. Zhang et al., 2008
		427 ± 10			
Grt–Ky (Sill) schist		454 ± 6		SHRIMP	J.X. Zhang et al., 2008
Grt–Ky (Sill) schist		**427 ± 10**			
Retrograde eclogite		452 ± 12		SHRIMP	Zhang et al., 2009
		430 ± 4			
Grt–Ky (Sill) schist	910–950	451–461	409 ± 12	SHRIMP	C. Zhang et al., 2009, 2012
		423 ± 12			Song et al., 2012
Yuka terrane					
Eclogite	750–800	**431 ± 4**		LA–ICP–MS	D.L. Chen et al., 2009; N.S. Chen et al., 2009
		436 ± 3			
Eclogite	847 ± 19	**433 ± 20**		SHRIMP	Song et al., 2010
Eclogite	847 ± 10			SIMS	Song et al., 2010
Metapelite	928 ± 4			SHRIMP	Song et al., 2012
Metapelite	996 ± 17			LA–ICP–MS	This study
Metapelite		**431 ± 3**	409 ± 4	LA–ICP–MS	D.L. Chen et al., 2009; N.S. Chen et al., 2009
Metapelite		**432 ± 19**		LA–ICP–MS	D.L. Chen et al., 2009; N.S. Chen et al., 2009
Metapelite		**426.5 ± 2.4**		LA–ICP–MS	This study
Lüliangshan					
Grt-lherzolite		**423 ± 6**	400–360	SHRIMP	Song et al., 2005a,b
Grt-harzburgite		**420 ± 6**		SHRIMP	Song et al., 2005a,b
Grt-pyroxenite			400 ± 12	SHRIMP	Song et al., 2005a,b
Grt-lherzolite		**427 ± 3**		SHRIMP	Xiong et al., 2011
Grt-pyroxinite		**429 ± 3**		SHRIMP	Xiong et al., 2011
Paragneiss		**430 ± 5**		LA–ICP–MS	Xiong et al., 2011
Grt-Ky schist		**427 ± 5**		LA–ICP–MS	Ma and Chen, 2006
Retrograde eclogite		448 ± 3		SHRIMP	J.X. Zhang et al., 2007b
		421 ± 5			

[a] Recalculated using weighted mean.

8.2.2. Oceanic subduction prior to continental collision—two stages of eclogite metamorphism

As described above, zircons from pelitic rocks in the Dulan terrane yielded fairly consistent HP-UHP metamorphic ages ranging from 431 ± 5 Ma to 423 ± 6 Ma (weighted mean). Eclogites in Dulan terrane, on the other hand, gave complicated metamorphic zircon ages in a wide range from 473 Ma to 422 Ma, which were interpreted to reflect HP/UHP conditions in eclogite-facies metamorphism (Song et al., 2003a, 2006; Mattinson et al., 2006b; G.B. Zhang et al., 2008; G.B. Zhang et al., 2009a,b; J.X. Zhang et al., 2010). The age range overlaps but extends much older than the 438–422 Ma ages of coesite-bearing zircons from eclogite and paragneiss (Song et al., 2006; Mattinson et al., 2009; J.X. Zhang et al., 2010; this study). These ages span a period of ~40 m.y. that might be too long for a single UHP metamorphic event of continental subduction, for example, duration of eclogitization is 10 Myr from 55 to 45 Ma in the Himalaya orogen (Guillot et al., 2008), UHP metamorphic ages of Dabie-Sulu terranes span a narrow range from 245 Ma to 225 Ma (e.g. Liu et al., 2006; Liu and Liou, 2011), and the orogeny spanning collision and HP-UHP metamorphism in the Western Gneiss Region have lasted for only 25 Myr from 425 Ma to 400 Ma (e.g., Hacker et al., 2003; Hacker, 2007).

Existence of UHP metamorphosed ophiolite sequence within the continental-type subduction belt demonstrated an oceanic subduction prior to the continental collision. It is ambiguous that some eclogites indeed formed during oceanic subduction, even though their protoliths are fragments of oceanic crust. Complexity of zircon ages of the Dulan eclogite may reflect multi-stages of HP-UHP metamorphic overprinting.

Ages in the histogram of the Dulan eclogite show two major peaks at 421 Ma and 445 Ma (Fig. 8F), representing two major metamorphic events, respectively. For some individual samples (Table 2), two stages of metamorphism can be clearly seen in terms of combining age data and CL images of zircon. Zircons from a Yematian eclogite (2D155) yielded 480 to 440 Ma with a weighted mean of 457 ± 7 Ma; one rim gave a 426 ± 12 Ma (Song et al., 2006). Mineral inclusions in the major domains are mainly Grt + Omp + Rt, rare quartz inclusions were also determined, suggesting HP metamorphism below coesite stability field.

For the individuals, although those eclogite samples (e.g., 2D73 of this study, Fig. 8) are very fresh with granoblastic grt + Omp + Rt and no retrograde overprinting, most zircon grains exhibit inner structure with strong luminescent, fir-tree zoned cores and weak luminescent rims in the CL images. The age 462 ± 13 Ma of cores and age 424 ± 13 Ma of rims indicate two stages of metamorphic growth in zircon in the eclogite. The core domain with HP mineral inclusions could well represent an HP metamorphic growth at eclogite-facies conditions, but the rim age cannot be explained by retrograde overprinting because the major rock-forming minerals still remain fresh. Garnet and Omp inclusions were also recognized in the rim domains (Figs. 6 and 7) and might indicate metamorphic growth at the UHP conditions, in spite of that no coesite inclusions were found. Consequently, two stages of HP-UHP metamorphism are distinct and the early HP stage from 445 Ma to 460 Ma (or earlier) can be interpreted to be time for oceanic subduction and the late (UHP) stage from 430 Ma to 420 Ma for continental subduction. And each single eclogite sample has recorded a complete history from oceanic subduction to continental subduction.

8.2.3. Granulite overprinting and decompression partial melting during exhumation

Granulite overprinting to UHPM rocks is well-developed in South Dulan belt and Xitieshan terrane. Through investigating eclogite and metapelite in the Lüliangshan region and Xitieshan terrane, Zhang J. and co-authors obtained zircon ages of 420–430 Ma from low-pressure metamorphic rocks (e.g. Grt–Sil schist) and retrograde eclogite. Therefore, they interpreted ages within the range of 420–435 Ma to be the time for granulite or amphibolite retrogression (Zhang et al., 2006; J.X. Zhang et al., 2007b; J.X. Zhang et al., 2008; J.X. Zhang et al., 2009a,b). However, eclogite retrogression with symplectite texture that partly or totally replaces Omp is generally interpreted as a decompression process from eclogite-facies to granulite-facies with slight temperature decrease (nearly identical). This texture is not equilibrium with garnet and zircons in this decompression are difficult to overgrow or recrystallize if no partial melting occurs (a good example is that zircons from the 950–910 Ma metapelites have experienced UHP metamorphism but hardly grown). Amphibolite overprinting also cannot make the previous eclogitic zircon totally recrystallized. Therefore, zircons from the amphibolite overprinting retrograde samples should be the ages of peak eclogite stage.

In the Dulan terrane, high P–T (P = 1.6–2.0 GPa and T = 860–950 °C) granulite occurs as blocks with adakitic melts in the South Dulan belt (Song et al., 2003a,b; Yu et al., 2009, 2012). Yu et al. (2010) reported zircon LA–ICP–MS ages of 447 ± 7 Ma from a high-pressure granulite and thus suggested it formed in the same ages as eclogites in the North Dulan Belt and had an independent history. In our samples, decompression texture and Omp inclusions in Kyanite (Song et al., 2003a,b) indicate that the mafic granulite is actually granulitized eclogite. Zircon crystals in the mafic granulite show complicated inner structure with multi-stage overgrowth; metamorphic cores with fir-tree sector zones gave ages of 439–474 Ma with a mean of 457 ± 10 Ma, the same as zircon SHRIMP ages of eclogite in the North Dulan belt (Song et al., 2006), and the dark luminescent magmatic rims (and newly formed crystals) gave a mean age of 404 ± 6 Ma (Song et al., in revision).

Zircons from adakitic melts yielded magma crystallization ages of 428–437 Ma by using LA–ICP–MS facility (Yu et al., 2012). These ages are overlapping zircon SHRIMP ages (430–438 Ma) from coesite-eclogites by J.X. Zhang et al. (2010). High-pressure tonalitic melts with assemblage of Grt + Ky + Ab + Qtz + Rt + Aln, on the other hand, yielded zircon SHRIMP age of 410 ± 4 Ma (Song et al., in revision).

These age results indicate that generation of adakitic melts is rather complicated and, if all data are reliable, has experienced for a long period of time. The forming age of the early adakitic magma overlaps the high-silica adakite (438 ± 6 Ma) in the west part of North Qilian orogen, which is believed to be formed by decompression melting of subducted slab (Chen et al., 2012). Reasonable interpretation is that decompression partial melting might occur during the exhumation of oceanic lithosphere in response to initiation of continental deep subduction.

8.2.4. Mountain building, UHP exhumation and decoupling of oceanic subduction zone and continent UHPM terranes

As indicated above, continental subduction will take place only with prior oceanic subduction of the leading edge of the oceanic lithosphere (the concept of passive margin connection). That is, convergence of one continent beneath another continues because the crust is still being pulled down by oceanic lithosphere sinking in the subduction zone. Therefore, from oceanic subduction to continental subduction should be necessarily a continuous process in the same subduction zone. However, continental-type (Alpine- or A-type) and oceanic-type (Pacific- or B-type) do not couple in the same belt as shown in the Himalayan orogen, where HP-UHPM belt occurs within High Himalaya crystalline sequence in Pakistan, India and Nepal (e.g., De Sigoyer et al., 2000; Mukherjee and Sachan, 2001; O'Brien et al., 2001) and is far away from the Indus-Yaluzangbo suture zone in the south. This phenomenon is most likely attributed to the different exhumation path and mechanism between the subducted oceanic and continent crusts, or to roll-back of subduction zone.

Unroofing and buoyancy were thought to be the major factors for exhumation of the UHPM continental crust from depths of 100–200 km (e.g., Ernst et al., 1997; Hacker et al., 2000), but they are not enough to explain decoupling of the oceanic and continental subduction zones. Convergence by underthrusting of one continent beneath another can pile up the front of the subducted crust and make the UHPM rocks diapiric rise along the subduction channel—a modal of 'two-way street' by Chopin (2003). This is the most likely exhumation path and can simply explain the tectonic pattern in the Early Paleozoic to be a united convergent zone from oceanic subduction (the North Qilian oceanic-type subduction zone) to continental subduction/collision (the North Qaidam UHPM belt).

8.2.5. Mountain collapse and extensional magmatism

Ancient orogens will inevitably be derooted and erosion at the post-orogenic stage. Tectonically adiabatic uplift by extensional collapse of orogen (e.g., Dewey, 1988) is responsible for decompression melting of the deeply subducted crust to generate S-type granite at ~400–390 Ma in the Dulan terrane, which is distinct from and later than adakites by partial melting of eclogite (see above). Continuous lithosphere extension and delamination resulted in strong magmatic activity and formed a number of diorite–granodiorite–granite plutons in the ages of ~400–360 Ma.

8.3. Tectonic evolution from oceanic subduction, to continental collision and to final mountain collapse

All materials in the North Qaidam UHPM belt records a complicated but integrated history that can be traced back to the assembly of the supercontinent Rodinia. It rifted again along the former Grenville-age orogenic belt and formed a new passive continental margin and an ocean basin namely the Qilian Ocean (e.g. Song et al., 2013). Therefore, two epochs of orogens, i.e., the Neoproterozoic (Grenvillian) and the Early Paleozoic (Caledonian), are involved in the subducted continental crust of the North Qaidam UHPM belt.

Several tectonic models have been proposed for evolution of the North Qaidam UHPM belt in the Paleozoic time (e.g., Yang et al., 2002a,b; Gehrels et al., 2003; Song et al., 2006, 2009c; Xu et al., 2006; Mattinson et al., 2007; Yin et al., 2007). Among these models, Yang et al. (2002a,b) suggested the North Qaidam UHPM belt and the North

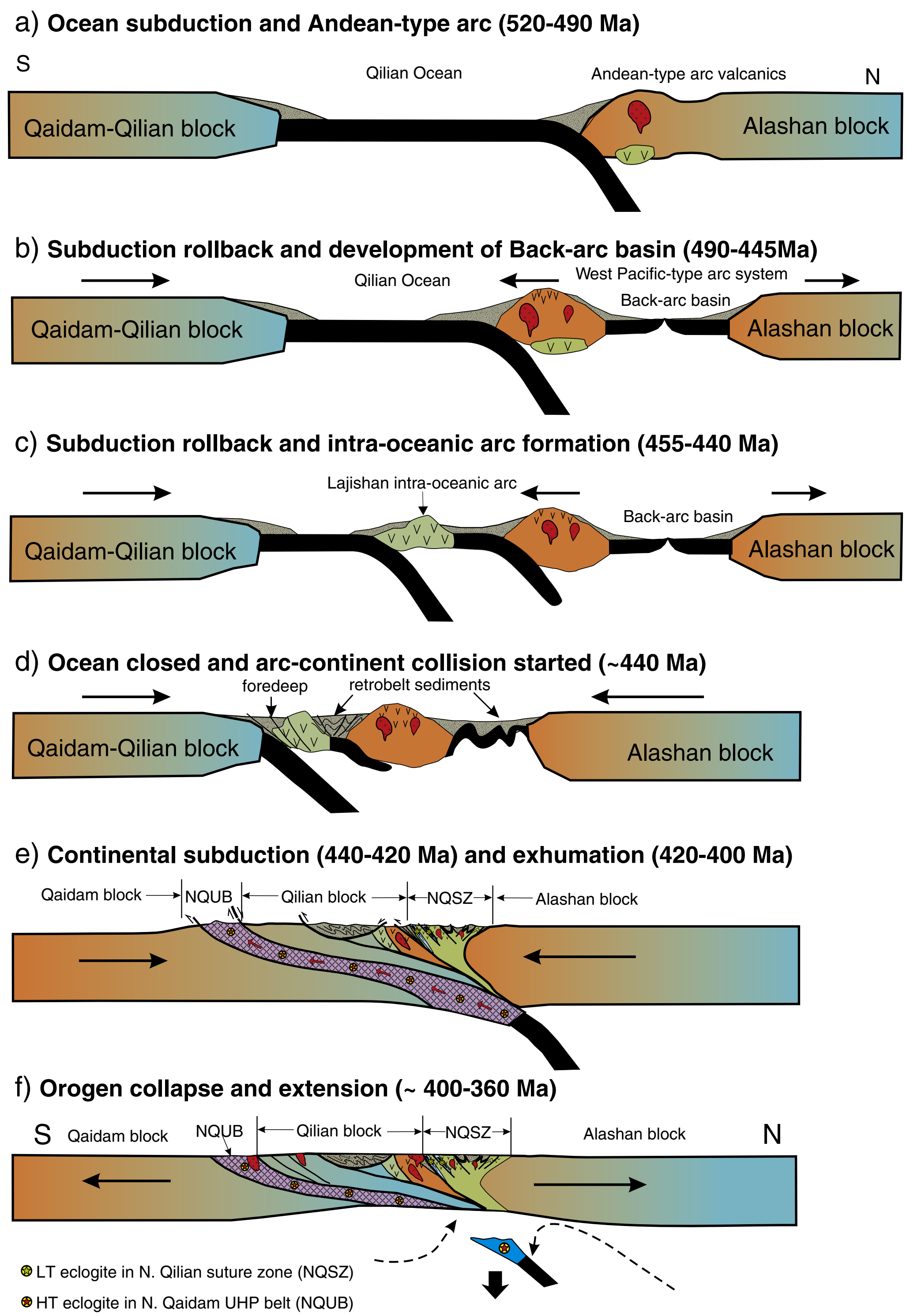

Fig. 19. Tectonic modal showing a complete orogeny from oceanic subduction, continental collision, subduction, mountain building, and to final extensional collapse inferred from the North Qaidam UHPM belt. Decoupling of oceanic suture zone and continental UHPM terranes occurs during continental collision and exhumation. Subduction rollback plays important roles in development of back-arc basin, intra-oceanic arc formation and continental collision.

Qilian oceanic-type suture zone are two independent subduction zones between Qaidam block and Qilian block and between Qilian block and Alashan block, respectively. Gehrels et al. (2003) proposed five possible models for the early Paleozoic tectonic evolution in the northern Tibetan plateau. However, as pointed above, continental subduction cannot take place without prior oceanic lithosphere subduction. And importantly, continental UHPM terranes cannot be confused with the oceanic suture zone, nor represent the boundary of two continents. Lines of evidence infer that the Qilian and Qaidam blocks on the two side of the North Qaidam UHPM belt are actually one fragment of the disintegrated Rodinia supercontinent (e.g. Li et al., 2008), and that the North Qaidam UHPM belt does not represent the convergence zone of two major continents (Song et al., 2006). On the basis of a comprehensive consideration of various aspects of geological evidence, we emphasize that the two sub-parallel belts (together with the Lajishan OIOAB) may represent a complete evolutionary sequence from oceanic subduction to continental collision. The North Qilian oceanic suture zone recorded a history from continental breakup to ocean basin evolution, and to the ultimate continental collision in the time period from the Neoproterozoic to the Paleozoic, whereas the North Qaidam UHPM belt exhibits a process from continental deep subduction, to mountain building and UHPM rock exhumation and to final mountain collapse as illustrated in Fig. 19.

In summary, seven major stages of tectonic evolution in this UHPM belt and associated region are briefly inferred as following.

1) Grenville-age orogenesis that resembled the supercontinent Rodinia at ~1300–900 Ma;
2) Rifting activity that broke up the supercontinent with continental flood basalts (CFBs) and granite intrusions at ~850–750 Ma
3) Opening and spreading of the Qilian Ocean at ~750–520 Ma;
4) Initiation of subduction at ~520 Ma, continental arc magmatism, extension of back-arc and SSZ ophiolite formation at ~490–445 Ma, and intra-oceanic arc volcanism at ~460–440 Ma, as results of subduction rollback (e.g., Lucente and Margheriti, 2008);
5) Closure of Qilian Ocean, continental collision between the Qaidam–Qilian block and the Alashan block, and continental deep subduction at ~440–420 Ma with peak UHP metamorphic ages at ~435–425 Ma, drived either by the former downgoing Qilian ocean slab (e.g., Wortel and Spakman, 2000) or by pushing down of the overriding upper plate (e.g., Doglioni et al., 2007). Some slabs might be partially molten due to thermo-disturbing in response to the continental subduction.
6) Uplift of mountain chain and exhumation of subducted crust with adakitic magma by decompression melting of eclogite as a result of slab breakoff at ~420–400. Decoupling of oceanic subduction zone and continental UHPM terranes is attributed to the different exhumation path and mechanism between the subducted oceanic and continent crusts, or to rollback of subduction zone.
7) Delamination and extensional collapse of the orogen with post-collisional granitic intrusions at ~ 400–360 Ma.

Acknowledgments

We thank C. Doglioni and S. Guillot for their constructive official review comments. This study was supported by the National Natural Science Foundation of China (Grant Nos. 41372060, 40825007, 41121062, 41130314), Basic Geological Survey Program of China Geological Survey (1212011121258), and the Major State Basic Research Development Projects (2009CB825007).

References

Brueckner, H.K., 1998. Sinking intrusion model from the emplacement of garnet-bearing peridotites into continent collision orogens. Geology 26, 631–634.

Brueckner, H.K., 2011. Geodynamics: double-dunk tectonics. Nat. Geosci. 4, 136–138.

Brueckner, H.K., Medaris, L.G., 2000. A general model for the intrusion and evolution of 'mantle' garnet peridotites in high-pressure and ultra-high-pressure metamorphic terranes. J. Metamorph. Geol. 18, 123–133.

Bundy, F.P., 1980. The P, T phase and reaction diamond for elemental carbon. J. Geophys. Res. 85, 6930–6936.

Cabanis, B., Lecolle, M., 1989. Le diagramme La/10-Y/15-Nb/8: Un outil pour la discrimination des series volcaniques et la mise en evidence des procesus de melange et/ou de contamination crutale. C. R. Acad. Sci. 309, 2023–2029.

Carswell, T., Compagnoni, R., 2003. Introduction with review of the definition, distribution and geotectonic significance of ultrahigh pressure metamorphism. In: Carswell, T., Compagnoni, R. (Eds.), Ultrahigh Pressure Metamorphism, EMU Notes in Mineralogy, Vol. 5, pp. 3–9.

Chen, D.L., Sun, Y., Liu, L., 2007a. In situ LA–ICP–MS zircon U–Pb age of ultrahigh-pressure eclogites in the Yukahe area, Northern margin of the Qaidam basin. Sci. China, Ser. D 37 (S1), 279–287.

Chen, D.L., Sun, Y., Liu, L., 2007b. The metamorphic ages of the country rock of the Yukahe eclogites in the North Qaidam and its geological significance. Earth Sci. Front. 14, 108–116.

Chen, D.L., Liu, L., Sun, Y., Liou, J.G., 2009a. Geochemistry and zircon U–Pb dating and its implications of the Yukahe HP/UHP terrane, the North Qaidam, NW China. J. Asian Earth Sci. 35, 259–272.

Chen, N.S., Gong, S.L., Sun, M., Li, X.Y., Xia, X.P., Wang, Q.Y., Wu, F.Y., Xu, P., 2009b. Precambrian evolution of the Quanji Block, northeastern margin of Tibet: insights from zircon U–Pb and Lu–Hf isotope compositions. J. Asian Earth Sci. 35, 367–376.

Chen, Y.X., Xia, X.H., Song, S.G., 2012. Petrogenesis of Aoyougou high-silica adakite in the North Qilian orogen, NW China: evidence for decompression melting of oceanic slab. Chin. Sci. Bull. 57, 2289–2301.

Chopin, C., 2003. Ultrahigh-pressure metamorphism: tracing continental crust into the mantle. Earth Planet. Sci. Lett. 212, 1–14.

Dan, W., Li, X.-H., Guo, J., Liu, Y., Wang, X.-C., 2012. Paleoproterozoic evolution of the eastern Alxa Block, westernmost North China: evidence from in situ zircon U–Pb dating and Hf–O isotopes. Gondwana Res. 21, 838–864.

Darby, B.J., Gehrels, G., 2006. Detrital zircon reference for the North China block. J. Asian Earth Sci. 26, 637–648.

de Sigoyer, J., Chavagnac, V., Blichert-Toft, J., Villa, I.M., Luais, B., Guillot, S., Cosca, M., Mascle, G., 2000. Dating the Indian continental subduction and collisional thickening in the northwest Himalaya: multichronology of the Tso Morari eclogites. Geology 28, 487–490.

DeCelles, P.G., Giles, K.A., 1996. Foreland basin systems. Basin Res. 8, 105–123.

Dewey, J.F., 1988. Extensional collapse of orogens. Tectonics 7, 1123–1139.

Dick, H.J.B., 1989. Abyssal periodotites, very slow spreading ridges and ocean ridge magmatism. In: Saunders, A.D., Norry, M.J., Saunders, A.D., Norry, M.J. (Eds.), Magmatism in the Ocean Basins. Geological Society, London, Special Publications, 42, pp. 71–105.

Dobrzhinetskaya, L., Green, H.W., Wang, S., 1996. Alpe Arami: a peridotite massif from depths of more than 300 kilometers. Science 271, 1841–1845.

Doglioni, C., 1994. Foredeeps versus subduction zones. Geology 22, 271–274.

Doglioni, C., Harabaglia, P., Merlini, S., Mongelli, F., Peccerillo, A., Piromallo, C., 1999. Orogens and slabs vs. their direction of subduction. Earth Sci. Rev. 45, 167–208.

Doglioni, C., Carminati, E., Cuffaro, M., 2006. Simple kinematics of subduction zones. Int. Geol. Rev. 48 (6), 479–493.

Doglioni, C., Carminati, E., Cuffaro, M., Scrocca, D., 2007. Subduction kinematics and dynamic constraints. Earth Sci. Rev. 83, 125–175.

Downes, H., 2001. Formation and modification of the shallow subcontinental lithospheric mantle: a review of geochemical evidence from ultramafic xenolith suites and tectonically emplaced ultramafic massifs of Western and Central Europe. J. Petrol. 42, 233–250.

Eckert, O.J., Newton, R.C., Kleppa, O.J., 1991. The DH of reaction and recalibration of garnet-pyroxene-plagioclasequartz geobarometers in the CMAS system by solution calorimetry. Am. Mineral. 76, 148–160.

Ernst, W.G., 2001. Subduction, ultrahigh-pressure metamorphism, and regurgitation of buoyant crustal slices—implications for arcs and continental growth. Phys. Earth Planet. Inter. 127, 253–275.

Ernst, W.G., Liou, J.G., 1995. Contrasting plate-tectonic styles of the Qinling-Dabie-Sulu and Franciscan metamorphic belts. Geology 23, 353–356.

Ernst, W.G., Maruyama, S., Wallis, S., 1997. Buoyancy-driven, rapid exhumation of ultrahigh-pressure metamorphosed continental crust. Proc. Natl. Acad. Sci. U. S. A. 94, 9532–9537.

Gehrels, G.E., Yin, A., Wang, X.-F., 2003. Detrital-zircon geochronology of the northeastern Tibetan plateau. Geol. Soc. Am. Bull. 115 (7), 881–896.

Geng, Y.-S., Wang, X.-S., Shen, Q.-H., Wu, C.-M., 2002. The discovery of Neoproterozoic Jinningian deformed granites in Alax area and its significance. Mineral. Petrogr. Acta 21, 412–420 (in Chinese with English abstract).

Geng, Y.-S., Wang, X.S., Shen, Q.H., Wu, C.M., 2006. Redefinition of the Alxa Group-complex (Precambrian metamorphic basement) in the Alxa area, Inner Mongolia. Geol. China 33, 138–145 (in Chinese with English abstract).

Guillot, S., Hattori, K., de Sigoyer, J., Nagler, T., Auzende, A.L., 2001. Evidence of hydration of the mantle wedge and its role in the exhumation of eclogites. Earth Planet. Sci. Lett. 193, 115–127.

Guillot, S., Maheo, G., de Sigoyer, J., Hattori, K., Pecher, A., 2008. Tethyan and Indian subduction viewed from the Himalayan High- to Ultra-High-Pressure metamorphic rocks in the Himalaya. Tectonophysics 451, 225–241.

Guillot, S., Hattori, K., Agard, P., Schwartz, S., Vidal, O., 2009. In: Lallemand, S., Funiciello, F. (Eds.), Exhumation Processes in Oceanic and Continental Subduction Contexts: A Review. Subduction Zone Dynamics. Springer-Verlag, Berlin Heidelberg, pp. 175–204. http://dx.doi.org/10.1007/978-3-540-87974-9.

Guo, J.J., Zhao, F.Q., Li, H.K., 1999. Jinningian collisional granite belt in the eastern sector of the Central Qilian Massif and its implication. Acta Geosci. Sin. 20, 10–15 (in Chinese with English abstract).

Hacker, B., 2007. Ascent of the ultrahigh-pressure Western Gneiss Region, Norway. Geol. Soc. Am. Spec. Pap. 419, 171–184.

Hacker, B.R., Ratschbacher, L., Webb, L., McWilliams, M.O., Ireland, T., Calvert, A., Dong, S., Wenk, H.-R., Chateigner, D., 2000. Exhumation of ultrahigh-pressure continental crust in East-central China: Late Triassic–Early Jurassic tectonic unroofing. J. Geophys. Res. 105, 13339–13364.

Hacker, B.R., Andersen, T.B., Root, D.B., Mehl, L., Mattinson, J.M., Wooden, J.L., 2003. Exhumation of high-pressure rocks beneath the Solund Basin, Western Gneiss Region of Norway. J. Metamorph. Geol. 21, 613–629.

Handy, M.R., M. Schmid, S., Bousquet, R., Kissling, E., Bernoulli, D., 2010. Reconciling plate-tectonic reconstructions of Alpine Tethys with the geological–geophysical record of spreading and subduction in the Alps. Earth Sci. Rev. 102, 121–158.

Hart, S.R., 1988. Heterogeneous mantle domains: signatures, genesis and micing chronologies. Earth Planet. Sci. Lett. 90, 273–296.

Hemingway, B.S., Bohlen, S.R., Hankins, W.B., Westrum, E.F., Kuskov, O.L., 1998. Heat capacity and thermodynamic properties for coesite and jadeite, reexamination of the quartz–coesite equilibrium boundary. Am. Mineral. 83, 409–418.

Herwartz, D., Nagel, T.J., Munker, C., Scherer, E.E., Froitzheim, N., 2011. Tracing two orogenic cycles in one eclogite sample by Lu–Hf garnet chronometry. Nat. Geosci. 4, 178–183.

Krogh, E.J., 1988. The garnet-clinopyroxene Fe-Mg-geothermometer – a reinterpretation of existing experimental data. Contrib. Mineral. Petrol. 99, 44–48.

Li, X.H., Su, L., Chung, S.L., Li, Z.X., Liu, Y., Song, B., Liu, D.Y., 2005. Formation of the Jinchuan ultramafic intrusion and the world's third largest Ni–Cu sulfide deposit: Associated with the similar to 825 Ma south China mantle plume? Geochem. Geophys. Geosyst. 6, Q11004. http://dx.doi.org/10.1029/2005GC001006.

Li, C., Zhai, Q., Dong, Y., Huang, X., 2006. Discovery of eclogite and its geological significance in Qiangtang area, central Tibet. Chin. Sci. Bull. 51, 1095–1100.

Li, Z.X., Bogdanova, S.V., Collins, A.S., Davidson, A., De Waele, B., Ernst, R.E., Fitzsimons, I.C.W., Fuck, R.A., Gladkochub, D.P., Jacobs, J., Karlstrom, K.E., Lu, S., Natapov, L.M., Pease, V., Pisarevsky, S.A., Thrane, K., Vernikovsky, V., 2008. Assembly, configuration, and breakup history of Rodinia: a synthesis. Precambrian Res. 160, 179–210.

Lindsley, D.H., 1983. Pyroxene thermometry. Am. Mineral. 68, 477–493.

Liou, J.G., Tsujimori, T., Zhang, R.Y., Katayama, I., Maruyama, S., 2004. Global UHP metamorphism and continental subduction/collision: the Himalayan model. Int. Geol. Rev. 46, 1–27.

Liou, J.G., Ernst, W., Song, S., Jahn, B.M., 2009. Tectonics and HP-UHP metamorphism of northern Tibet—preface. J. Asian Earth Sci. 35, 191–198.

Liu, F.L., Liou, J.G., 2011. Zircon as the best mineral for P–T–time history of UHP metamorphism: a review on mineral inclusions and U–Pb SHRIMP ages of zircons from the Dabie–Sulu UHP rocks. J. Asian Earth Sci. 40, 1–39.

Liu, D.Y., Jian, P., Kröner, A., Xu, S.T., 2006. Dating of prograde metamorphic events deciphered from episodic zircon growth in rocks of the Dabie–Sulu UHP complex, China. Earth Planet. Sci. Lett. 250, 650–666.

Liu, L., Wang, C., Cao, Y.T., Chen, D.L., Kang, L., Yang, W.Q., Zhu, X.H., 2012a. Geochronology of multi-stage metamorphic events: constraints on episodic zircon growth from the UHP eclogite in the South Altyn, NW China. Lithos 136, 10–26.

Liu, X.C., Wu, Y.B., Gao, S., Liu, Q., Wang, H., Qin, Z.W., Li, Q.L., Li, X.H., Gong, H.J., 2012b. First record and timing of UHP metamorphism from zircon in the Xitieshan terrane: implications for the evolution of the entire North Qaidam metamorphic belt. Am. Mineral. 97, 1083–1093.

Lu, S.N., 2002. Preliminary Study of Precambrian Geology in the North Tibet–Qinghai Plateau. Geological Publishing House, Beijing (125 pp. (in Chinese)).

Lucente, F.P., Margheriti, L., 2008. Subduction rollback, slab breakoff, and induced strain in the uppermost mantle beneath Italy. Geology 36, 375–378.

Ludwig, K.R., 1991. ISOPLOT: a plotting and regression program for radiogenicisotope data. USGS Open-file Report 91-445, pp. 1–39.

Ma, X.D., Chen, D.L., 2006. LA–ICP–MS zircon U–Pb dating of quartzo-feldspathic gneisses—the country rocks of ultrahigh-pressure metamorphic rocks on the northern margin of the Qaidam basin, Northwest China. Geol. Bull. China 25, 99–103.

Maruyama, S., Liou, J.G., Terabayashi, M., 1996. Blueschists and eclogites of the world and their exhumation. Int. Geol. Rev. 38, 485–594.

Mattinson, C.G., Wooden, J.L., Liou, J.G., Bird, D.K., Wu, C.L., 2006a. Age and duration of eclogite-facies metamorphism, North Qaidam HP/UHP terrane, western China. Am. J. Sci. 306, 683–711.

Mattinson, C.G., Wooden, J.L., Liou, J.G., Bird, D.K., Wu, C.L., 2006b. Geochronology and tectonic significance of Middle Proterozoic granitic orthogneiss, North Qaidam HP/UHP terrane, Western China. Mineral. Petrol. 88, 227–241.

Mattinson, C.G., Menold, C.A., Zhang, J.X., Bird, D.K., 2007. High- and ultrahigh-pressure metamorphism in the North Qaidam and South Altyn Terranes, western China. Int. Geol. Rev. 49, 969–995.

Mattinson, C.G., Wooden, J.L., Zhang, J., Bird, D.K., 2009. Paragneiss zircon geochronology and trace element geochemistry, North Qaidam HP/UHP terrane, western China. J. Asian Earth Sci. 35, 298–309.

Medaris, L.M., Carswell, D.A., 1990. Petrogenesis of Mg–Cr garnet peridotites in European metamorphic belts. In: Carswell, D.A. (Ed.), Eclogite Facies Rocks. Blackie, Glasgow, pp. 260–291.

Menold, C.A., Manning, C.E., Yin, A., Tropper, P., Chen, X.-H., Wang, X.-F., 2009. Metamorphic evolution, mineral chemistry and thermobarometry of orthogneiss hosting ultrahigh-pressure eclogites in the North Qaidam metamorphic belt, Western China. J. Asian Earth Sci. 35, 273–284.

Mukherjee, B.K., Sachan, H.K., 2001. Discovery of coesite from Indian Himalaya: a record of ultrahigh pressure metamorphism in Indian continental crust. Curr. Sci. 81, 1358–1361.

Niu, Y., 1999. Comments on some misconceptions in igneous and experimental petrology and methodology: a reply. J. Petrol. 40, 1195–1203.

O'Brien, P.J., Zotov, N., Law, R., Khan, M.A., Jan, M.Q., 2001. Coesite in Himalayan eclogite and implications for models of India–Asia collision. Geology 29, 435–438.

Powell, R., 1985. Regression diagnostics and robust regression in geothermometer/geobarometer calibration: the garnet-clinopyroxene geothermometer revisited. J. Metamorph. Geol. 3, 231–243.

Ravna, E.J.K., Terry, M.P., 2004. Geothermobarometry of UHP and HP eclogites and schists—an evaluation of equilibria among garnet–clinopyroxene–kyanite–phengite–coesite / quartz. J. Metamorph. Geol. 22, 579–592.

Ren, J.S., Jiang, C.F., Zhang, Z.K., 1980. Geotectonics and Evolution of China. Science Press, Beijing 1–140 (in Chinese).

Royden, L.H., Burchfiel, B.C., Van der Hilst, R.D., 2008. The geologic evolution of the Tibetan Plateau. Science 321, 1054–1058.

Rubatto, D., Regis, D., Hermann, J., Boston, K., Engi, M., Beltrando, M., McAlpine, S.R.B., 2011. Yo-yo subduction recorded by accessory minerals in the Italian Western Alps. Nat. Geosci. 4, 338–342.

Shi, R.D., Griffin, W.L., O'Reilly, S.Y., Zhao, G.C., Huang, Q.S., Li, J., Xu, J.F., 2010. Evolution of the Lüliangshan garnet peridotites in the North Qaidam UHP belt, Northern Tibetan Plateau: constraints from Re–Os isotopes. Lithos 117, 307–321.

Song, S.G., Yang, J.S., 2001. Sanidine + quartz inclusions in Dulan Eclogites: evidence for UHP metamorphism on the north margin of the Qaidam Basin, NW China. Acta Geol. Sin. 75, 180–185 (in Chinese with English abstract).

Song, S.G., Yang, J.S., Xu, Z.Q., Liou, J.G., Wu, C.L., Shi, R.D., 2003a. Metamorphic evolution of coesite-bearing UHP terrane in the North Qaidam, northern Tibet, NW China. J. Metamorph. Geol. 21, 631–644.

Song, S.G., Yang, J.S., Liou, J.G., Wu, C.L., Shi, R.D., Xu, Z.Q., 2003b. Petrology, geochemistry and isotopic ages of eclogites in the Dulan UHPM terrane, the North Qaidam, NW China. Lithos 70 (3–4), 195–211.

Song, S.G., Zhang, L.F., Niu, Y., 2004. Ultra-deep origin of garnet peridotite from the North Qaidam ultrahigh-pressure belt, Northern Tibetan Plateau, NW China. Am. Mineral. 89, 1330–1336.

Song, S.G., Zhang, L.F., Chen, J., Liou, J.G., Niu, Y.L., 2005a. Sodic amphibole exsolutions in garnet from garnet–peridotite, North Qaidam UHPM belt, NW China: implications for ultradeep-origin and hydroxyl defects in mantle garnets. Am. Mineral. 90, 814–820.

Song, S.G., Zhang, L.F., Niu, Y.L., Su, L., Jian, P., Liu, D.Y., 2005b. Geochronology of diamond-bearing zircons from garnet peridotite in the North Qaidam UHPM belt, Northern Tibetan Plateau: a record of complex histories from oceanic lithosphere subduction to continental collision. Earth Planet. Sci. Lett. 234, 99–118.

Song, S.G., Zhang, L.F., Niu, Y.L., Su, L., Song, B.A., Liu, D.Y., 2006. Evolution from oceanic subduction to continental collision: a case study from the Northern Tibetan Plateau based on geochemical and geochronological data. J. Petrol. 47, 435–455.

Song, S.G., Su, L., Niu, Y., Zhang, L.F., 2007a. Petrological and geochemical constraints on the origin of garnet peridotite in the North Qaidam ultrahigh-pressure metamorphic belt, Northwestern China. Lithos 96, 243–265.

Song, S.G., Zhang, L.F., Niu, Y.L., Wei, C.J., Liou, J.G., Shu, G.M., 2007b. Eclogite and carpholite-bearing meta-pelite in the North Qilian suture zone, NW China: implications for Paleozoic cold oceanic subduction. J. Metamorph. Geol. 25, 547–563.

Song, S.G., Niu, Y.L., Zhang, L.F., Wei, C.J., Liou, J.G., Su, L., 2009a. Tectonic evolution of early Paleozoic HP metamorphic rocks in the North Qilian Mountains, NW China: new perspectives. J. Asian Earth Sci. 35, 334–353.

Song, S.G., Niu, Y.L., Zhang, G.B., Zhang, L.F., 2009b. Two types of peridotite in North Qaidam UHPM belt and their tectonic implications for oceanic and continental subduction: a review. J. Asian Earth Sci. 35, 285–297.

Song, S.G., Niu, Y.L., Zhang, L.F., Zhang, G.B., 2009c. Time constraints on orogenesis from oceanic subduction to continental subduction, collision, and exhumation: an example from North Qilian and North Qaidam HP-UHP belts. Acta Petrol. Sin. 25, 2067–2077.

Song, S.G., Niu, Y.L., Zhang, L.F., Bucher, K., 2009d. The Lüliangshan garnet peridotite massif of the North Qaidam UHPM belt, NW China—a review of its origin and metamorphic evolution. J. Metamorph. Geol. 27, 621–638.

Song, S.G., Su, L., Niu, Y.L., 2009e. Generation of adakite: melting of eclogite during exhumation of UHPM terrane. Geochim. Cosmochim. Acta 73, A1252.

Song, S.G., Su, L., Li, X.-h, Zhang, G.B., Niu, Y.L., Zhang, L.F., 2010. Tracing the 850-Ma continental flood basalts from a piece of subducted continental crust in the North Qaidam UHPM belt, NW China. Precambrian Res. 183, 805–816.

Song, S.G., Zhang, C., Li, X.H., 2011. HP/UHP metamorphic time of eclogite in the Xitieshan terrane, North Qaidam UHPM belt, NW China. Acta Petrol. Sin. 27 (4), 1191–1197.

Song, S.G., Su, L., Li, X.H., Niu, Y.L., Zhang, L.F., 2012. Grenville-age orogenesis in the Qaidam–Qilian block: the link between South China and Tarim. Precambrian Res. 220, 9–22.

Song, S.G., Niu, Y.L., Su, L., Xia, X.H., 2013. Tectonics of the North Qilian orogen, NW China. Gondwana Res. 23, 1378–1401.

Song, S.G., Niu, Y.L., Su L., Wei, C.J., Zhang, L.F., Generation of tonalitic-trondhjemitic (adakitic) magmas: Melting of eclogite during exhumation of the UHP metamorphic terrane. Geochim. Cosmochim. Acta, in revision.

Spengler, D., van Roermund, H.L.M., Drury, M.R., Ottolini, L., Mason, P.R.D., Davies, G.R., 2006. Deep origin and hot melting of an Archaean orogenic peridotite massif in Norway. Nature 440, 913–917.

Streckeisten, A., 1976. To each plutonic rock its proper name. Earth Sci. Rev. 1, 1–33.

Tapponnier, P., Xu, Z., Roger, F., Meyer, B., Arnaud, N., Wittlinger, G., Yang, J.S., 2001. Oblique stepwise rise and growth of the Tibet Plateau. Science 294, 1671–1677.

Thomas, W.A., 1983. Continental margins, orogenic belts, and intracratonic structures. Geology 11, 270–272.

Torsvik, T.H., Smethurst, M.A., Meert, J.G., Van der Voo, R., McKerrow, W.S., Brasier, M.D., Sturt, B.A., Walderhaug, H.J., 1996. Continental break-up and collision in the Neoproterozoic and Palaeozoic—a tale of Baltica and Laurentia. Earth Sci. Rev. 40, 229–258.

Tung, K.A., Yang, H.Y., Liu, D.Y., 2007a. SHRIMP U–Pb geochronology of detrital zircons from the Longshoushan Group and its tectonic significance. Chin. Sci. Bull. 52, 1414–1425.

Tung, K.A., Yang, H.J., Yang, H.Y., Liu, D.Y., Zhang, J.X., Wan, Y.S., Tseng, C.Y., 2007b. SHRIMP U–Pb geochronology of the zircons from the Precambrian basement of the Qilian Block and its geological significances. Chin. Sci. Bull. 52, 2687–2701.

van Roermund, H.L.M., Drury, M.R., 1998. Ultra-high pressure (P > 6 GPa) garnet peridotites in Western Norway: exhumation of mantle rocks from >185 km depth. Terra Nova 10, 295–301.

van Roermund, H.L.M., Drury, M.R., Barnhoorn, A., de Ronde, A., 2001. Non-silicate inclusions in garnet from an ultra-deep orogenic peridotite. Geol. J. 35, 209–229.

Vielzeuf, D., Schmidt, M.W., 2001. Melting relations in hydrous systems revisited: application to metapeleties, metagreywackes and metabasalts. Contrib. Mineral. Petrol. 141, 251–267.

Wan, Y.S., Xu, Z.Q., Yang, J.S., 2001. Ages and compositions of the Precambrian high-grade basement of the Qilian terrance and its adjacent areas. Acta Geol. Sin. 75, 375–384.

Wan, Y.S., Zhang, J.X., Yang, J.S., Xu, Z.Q., 2006. Geochemistry of high-grade metamorphic rocks of the North Qaidam Mountains and their geological significance. J. Asian Earth Sci. 28, 174–184.

Wang, H.C., Yuan, G.B., Xin, H.T., Hao, G.J., Zhang, H.B., Wang, Q.H., Tian, Q., 2004. Geological characteristic and age of the Iqe River Group-complex on the northern margin of the Qaidam basin. Geol. Bull. China 23, 314–321 (in Chinese with English abstract).

Wang, Q.Y., Pan, Y.M., Chen, N.S., Li, X.Y., Chen, H.H., 2009. Proterozoic polymetamorphism in the Quanji Block, northwestern China: evidence from microtextures, garnet compositions and monazite CHIME ages. J. Asian Earth Sci. 34, 686–698.

Whitney, D.L., Evans, B.W., 2010. Abbreviations for names of rock-forming minerals. Am. Mineral. 95, 185–187.

Winchester, J.A., Floyd, P.A., 1977. Geochemical discrimination of different magma series and their differentiation products using immobile elements. Geochem. Geol. 20, 325–343.

Wortel, M.J.R., Spakman, W., 2000. Subduction and slab detachment in the Mediterranean–Carpathian region. Science 290, 1910–1917.

Wu, H.Q., Feng, Y.M., Song, S.G., 1993. Metamorphism and deformation of blueschist belts and their tectonic implications, North Qilian Mountains, China. J. Metamorph. Geol. 11, 523–536.

Wu, C., Yang, J., Wooden, J.L., 2004. Zircon U–Pb SHRIMP dating of the Yematan Batholith in Dulan, north Qaidam, NW China. Chin. Sci. Bull. 49, 1736–1740.

Wu, C.L., Gao, Y.H., Wu, S.P., Chen, Q.P., Wooden, J.L., Mazadab, F.K., Mattinson, C., 2007. Zircon SHRIMP U–Pb dating of granites from the Da Qaidam area in the north margin of Qaidam Basin, NW China. Acta Petrol. Sin. 23, 1861–1875.

Xia, X.H., Song, S.G., Niu, Y.L., 2012. Tholeiite–Boninite terrane in the North Qilian suture zone: implications for subduction initiation and back-arc basin development. Chem. Geol. 328, 259–277.

Xiong, Q., Zheng, J., Griffin, W.L., O'Reilly, S.Y., Zhao, J., 2011. Zircons in the Shenglikou ultrahigh-pressure garnet peridotite massif and its country rocks from the North Qaidam terrane (western China): Meso-Neoproterozoic crust–mantle coupling and early Paleozoic convergent plate-margin processes. Precambrian Res. 187, 33–57.

Xiong, Q., Zheng, J., Griffin, W.L., O'Reilly, S.Y., Pearson, N.J., 2012. Decoupling of U–Pb and Lu–Hf isotopes and trace elements in zircon from the UHP North Qaidam orogen, NE Tibet (China): tracing the deep subduction of continental blocks. Lithos 155, 125–145.

Xu, Z.Q., Yang, J.S., Wu, C.L., Li, H.B., Zhang, J.X., Qi, X.X., Song, S.G., Qiu, H.J., 2006. Timing and mechanism of formation and exhumation of the Northern Qaidam ultrahigh-pressure metamorphic belt. J. Asian Earth Sci. 28, 160–173.

Yang, J.J., Powell, R., 2008. Ultrahigh-pressure garnet peridotites from the devolatilization of sea-floor hydrated ultramafic rocks. J. Metamorph. Geol. 26, 695–716.

Yang, J.J., Zhu, H., Deng, J.F., Zhou, T.Z., Lai, S.C., 1994. Discovery of garnet-peridotite at the northern margin of the Qaidam Basin and its significance. Acta Petrol. Mineral. 13, 97–105 (in Chinese with English abstract).

Yang, J.S., Xu, Z.Q., Li, H.B., Wu, C.L., Cui, J.W., Zhang, J.X., Chen, W., 1998. Discovery of eclogite at northern margin of Qaidam basin, NW China. Chin. Sci. Bull. 43, 1755–1760.

Yang, J.S., Xu, Z.Q., Song, S.G., Zhang, J.X., Wu, C.L., Shi, R.D., Li, H.B., Brunel, M., 2001. Discovery of coesite in the North Qaidam Early Palaeozoic ultrahigh pressure (UHP) metamorphic belt, NW China. C. R. Acad. Sci. II Fascicule Sci. Terre Planets 333, 719–724.

Yang, J.S., Xu, Z.Q., Song, S.G., Zhang, J.X., Wu, C.L., Shi, R.D., Li, H.B., Brunel, M., Tapponnier, P., 2002a. Subduction of continental crust in the early palaeozoic North Qaidam ultrahigh-pressure metamorphic belt, NW China: evidence from the discovery of coesite in the belt. Acta Geol. Sin. Engl. Ed. 76, 63–68.

Yang, J.S., Xu, Z.Q., Zhang, J.X., Song, S.G., Wu, C.L., Shi, R.D., Li, H.B., Brunel, M., 2002b. Early Palaeozoic North Qaidam UHP metamorphic belt on the north-eastern Tibetan plateau and a paired subduction model. Terra Nova 14, 397–404.

Yang, J.S., Wu, C.L., Zhang, J.X., Shi, R.D., Meng, F.C., Wooden, J., Yang, H.Y., 2006. Protolith of eclogites in the north Qaidam and Altun UHP terrane, NW China: earlier oceanic crust? J. Asian Earth Sci. 28, 185–204.

Yin, A., Manning, C.E., Lovera, O., Menold, C.A., Chen, X., Gehrels, G.E., 2007. Early Paleozoic tectonic and thermomechanical evolution of ultrahigh-pressure (UHP) metamorphic rocks in the Northern Tibetan Plateau, Northwest China. Int. Geol. Rev. 49, 681–716.

Yin, A., Dang, Y.Q., Wang, L.C., Jiang, W.M., Zhou, S.P., Chen, X.H., Gehrels, G.E., McRivette, M.W., 2008a. Cenozoic tectonic evolution of Qaidam basin and its surrounding regions (part 1): the southern Qilian Shan–Nan Shan thrust belt and northern Qaidam basin. Geol. Soc. Am. Bull. 120, 813–846.

Yin, A., Dang, Y.Q., Zhang, M., Chen, X.H., McRivette, M.W., 2008b. Cenozoic tectonic evolution of Qaidam basin and its surrounding regions (part 2): structural geology, sedimentation and regional tectonic reconstruction. Geol. Soc. Am. Bull. 120, 847–876.

Yu, S.Y., Zhang, J.X., Li, J.P., 2009. Metamorphism history and dynamics of high-pressure granulites in the Dulan area of the North Qaidam Mountains, northwest China. Acta Petrol. Sin. 25, 2224–2234 (in Chinese with English abstract).

Yu, S.Y., Zhang, J.X., Del Real, P.D., 2010. Petrology and P–T path of high-pressure granulite from the Dulan area, North Qaidam Mountains, northwestern China. J. Asian Earth Sci. 42, 641–660.

Yu, S., Zhang, J., Del Real, P.G., 2012. Geochemistry and zircon U–Pb ages of adakitic rocks from the Dulan area of the North Qaidam UHP terrane, north Tibet: constraints on the timing and nature of regional tectonothermal events associated with collisional orogeny. Gondwana Res. 21, 167–179.

Zhai, Q.G., Zhang, R.Y., Jahn, B.M., Li, C., Song, S.G., Wang, J., 2011. Triassic eclogites from central Qiangtang, northern Tibet, China: petrology, geochronology and metamorphic P–T path. Lithos 125, 173–189.

Zhang, J.X., Zhang, Z.M., Xu, Z.Q., Yang, J.S., Cui, J.W., 2001. Petrology and geochronology of eclogites from the western segment of the Altyn Tagh, Northwestern China. Lithos 56, 187–206.

Zhang, G.B., Song, S.G., Zhang, L.F., Niu, Y., Shu, G.M., 2005a. Ophiolite-type mantle peridotite from Shaliuhe, North Qaidam UHPM belt, NW China and its tectonic implications. Acta Petrol. Sin. 21, 1049–1058.

Zhang, J.X., Yang, J.S., Mattinson, C.G., Xu, Z.Q., Meng, F.C., Shi, R.D., 2005b. Two contrasting eclogite cooling histories, North Qaidam HP/UHP terrane, western China: petrological and isotopic constraints. Lithos 84, 51–76.

Zhang, J.X., Yang, J.S., Meng, F.C., Wan, Y.S., Li, H.M., Wu, C.L., 2006. U–Pb isotopic studies of eclogites and their host gneisses in the Xitieshan area of the North Qaidam mountains, western China: new evidence for an early Paleozoic HP-UHP metamorphic belt. J. Asian Earth Sci. 28, 143–150.

Zhang, J.X., Meng, F.C., Wan, Y.S., 2007a. A cold Early Palaeozoic subduction zone in the North Qilian Mountains, NW China: petrological and U–Pb geochronological constraints. J. Metamorph. Geol. 25, 285–304.

Zhang, J.X., Meng, F.C., Yu, S.Y., 2007b. Metamorphic history recorded in high pressure mafic granulites in the Lüliangshan Mountains to the north of Qaidam Basin, northwest China: evidence from petrology and zircon SHRIMP geochronology. Earth Sci. Front. 2007 (14), 85–97.

Zhang, G.B., Song, S.G., Zhang, L.F., Niu, Y.L., 2008a. The subducted oceanic crust within continental-type UHP metamorphic belt in the North Qaidam, NW China: evidence from petrology, geochemistry and geochronology. Lithos 104, 99–118.

Zhang, J.X., Mattinson, C.G., Meng, F.C., Wan, Y.S., Tung, K., 2008b. Polyphase tectonothermal history recorded in granulitized gneisses from the North Qaidam HP/UHP metamorphic terrane, Western China: evidence from zircon U–Pb geochronology. Geol. Soc. Am. Bull. 120, 732–749.

Zhang, C., Zhang, L.F., Zhang, G.B., Song, S.G., 2009a. Petrology and calculation of retrograde PT path of eclogites from Xitieshan, North Qaidam, China. Acta Petrol. Sin. 25, 2247–2259.

Zhang, G.B., Ellis, D.J., Christy, A.G., Zhang, L.F., Niu, Y.L., Song, S.G., 2009b. UHP metamorphic evolution of coesite-bearing eclogite from the Yuka terrane, North Qaidam UHPM belt, NW China. Eur. J. Mineral. 21, 1287–1300.

Zhang, G.B., Zhang, L.F., Song, S.G., 2009c. UHP metamorphic evolution and SHRIMP geochronology of a metaophiolitic gabbro in the North Qaidam, NW China. J. Asian Earth Sci. 35, 310–322.

Zhang, J.X., Meng, F.C., Li, J.P., Mattinson, C.G., 2009d. Coesite in eclogite from the north Qaidam Mountains and its implication. Chin. Sci. Bull. 54, 1105–1110.

Zhang, J.X., Mattinson, C.G., Meng, F.C., Yang, H.J., Wan, Y.S., 2009e. U–Pb geochronology of paragneisses and metabasite in the Xitieshan area, north Qaidam Mountains, western China: constraints on the exhumation of HP/UHP metamorphic rocks. J. Asian Earth Sci. 35, 245–258.

Zhang, R.Y., Liou, J.G., Iizuka, Y., Yang, J.S., 2009f. First record of K-cymrite in North Qaidam UHP eclogite, Western China. Am. Mineral. 94, 222–228.

Zhang, G.B., Ellis, D.J., Christy, A.G., Zhang, L.F., Song, S.G., 2010a. Zr-in-rutile thermometry in eclogites from Western China. Contrib. Mineral. Petrol. 160, 427–439.

Zhang, J.X., Mattinson, C.G., Yu, S.Y., Li, J.P., Meng, F.C., 2010b. U–Pb zircon geochronology of coesite-bearing eclogites from the southern Dulan area of the North Qaidam UHP terrane, northwestern China: spatially and temporally extensive UHP metamorphism during continental subduction. J. Metamorph. Geol. 28, 955–978.

Zhang, C., Zhang, L., Roermund, H.V., Song, S., Zhang, G., 2011. Petrology and SHRIMP U–Pb dating of Xitieshan eclogite, North Qaidam UHP metamorphic belt, NW China. J. Asian Earth Sci. 42, 752–767.

Zhang, C., Van Roermund, H., Zhang, L.F., Spiers, C., 2012. A polyphase metamorphic evolution for the Xitieshan paragneiss of the north Qaidam UHP metamorphic belt, western China: In-situ EMP monazite- and U–Pb zircon SHRIMP dating. Lithos 136, 27–45.

Zhao, G.C., Sun, M., Wilde, S.A., Li, S.Z., 2005. Late Archean to Paleoproterozoic evolution of the North China Craton: key issues revisited. Precambrian Res. 136, 177–202.